water

MDPI

Review

Heterogenization of Molecular Water Oxidation Catalysts in Electrodes for (Photo)Electrochemical Water Oxidation

Carla Casadevall

Yusuf Hamied Department of Chemistry, University of Cambridge, Lensfield Road, Cambridge CB21EW, UK; cc2036@cam.ac.uk

Abstract: Water oxidation is still one of the most important challenges to develop efficient artificial photosynthetic devices. In recent decades, the development and study of molecular complexes for water oxidation have allowed insight into the principles governing catalytic activity and the mechanism as well as establish ligand design guidelines to improve performance. However, their durability and long-term stability compromise the performance of molecular-based artificial photosynthetic devices. In this context, heterogenization of molecular water oxidation catalysts on electrode surfaces has emerged as a promising approach for efficient long-lasting water oxidation for artificial photosynthetic devices. This review covers the state of the art of strategies for the heterogenization of molecular water oxidation catalysts onto electrodes for (photo)electrochemical water oxidation. An overview and description of the main binding strategies are provided explaining the advantages of each strategy and their scope. Moreover, selected examples are discussed together with the the differences in activity and stability between the homogeneous and the heterogenized system when reported. Finally, the common design principles for efficient (photo)electrocatalytic performance summarized.

Keywords: water oxidation; heterogenized catalysts; (photo)electrochemical water oxidation; electrocatalysis

check for updates

Citation: Casadevall, C. Heterogenization of Molecular Water Oxidation Catalysts in Electrodes for (Photo)Electrochemical Water Oxidation. *Water* **2022**, *14*, 371. https://doi.org/10.3390/w14030371

Academic Editor: Joaquín Soriano-López

Received: 6 January 2022
Accepted: 24 January 2022
Published: 26 January 2022

Publisher's Note: MDPI stays neutral with regard to jurisdictional claims in published maps and institutional affiliations.

Copyright: © 2022 by the author. Licensee MDPI, Basel, Switzerland. This article is an open access article distributed under the terms and conditions of the Creative Commons Attribution (CC BY) license (https://creativecommons.org/licenses/by/4.0/).

1. Introduction

1.1. Energy Challenge, Natural and Artificial Photosynthesis

In recent decades, the need to mitigate the increasing CO_2 emissions and transition to a sustainable society has increased in importance due to the high anthropogenic CO_2 emissions that have caused 1.1 °C of global warming. Indeed, at the current rate of energy consumption, this scenario is likely to reach 1.5 °C of global warming by 2050 [1]. In this line, the sustainable synthesis of fuels and chemicals using CO_2 and water as abundant primary feedstock, and the widespread and unlimited sunlight as driving energy, provides a potential feasible pathway toward a greener chemical industry and society [2,3], despite being very challenging at the same time [4,5].

In this context, nature, upon million years of evolution, has provided photosynthetic organisms with a very complex and elegant machinery that allows them to sustain their life by solely using sunlight, CO_2 and water to generate their fuel and source or energy (carbohydrates, producing only O_2 as byproduct) via so called natural photosynthesis [6,7]. During natural photosynthesis, solar energy is harnessed into the chemical bonds of carbohydrates such as glucose. This process takes place in the thylakoid membranes of chloroplasts and is possible due to the orchestration and synchronized cooperation of photosystem II (PSII) and photosystem I (PSI) together with other membrane protein complexes and carriers present in the chloroplasts [8,9]. During natural photosynthesis, light excitation of the chlorophyll pigments present in PSII triggers the oxidation of a tetranuclear manganese cluster which is the active center of the oxygen evolving complex (OEC), which upon four electron oxidations is able to oxidize the molecule of water to generate O_2 while releasing

protons and electrons. These reductive equivalents are transferred to the reductive site by cytochrome b6f to PSI (electron transport chain or Z scheme), where they are separated to generate the reduced molecule NADPH by a ferredoxin-$NADP^+$ reductase (FNR), and the proton gradient triggers the APT production by the ATP synthase. Finally, these reductive equivalents and energy molecules (NADPH and ATP, respectively) are used in the Calvin cycle to reduce CO_2 to carbohydrates (CO_2 fixation) (Scheme 1) [6,7]. Alternatively, in some organisms, hydrogenase enzymes use the released electron from the oxidation of water to reduce protons to hydrogen, which can be directly used as fuel. Despite the fact that the mechanism of photosynthesis is not fully unraveled, a key feature of natural photosynthesis is that it spatially arranges and orientates reaction centers and light harvesters along the thylakoid membrane of chloroplasts, separating the reduction form the oxidation side, minimizing cross-reactivity. Therefore, mimicking and understanding how natural photosynthesis operates and transfers primary energy vectors to harness solar energy into molecules are essential to develop efficient catalytic systems to produce solar fuels and chemicals [10–12].

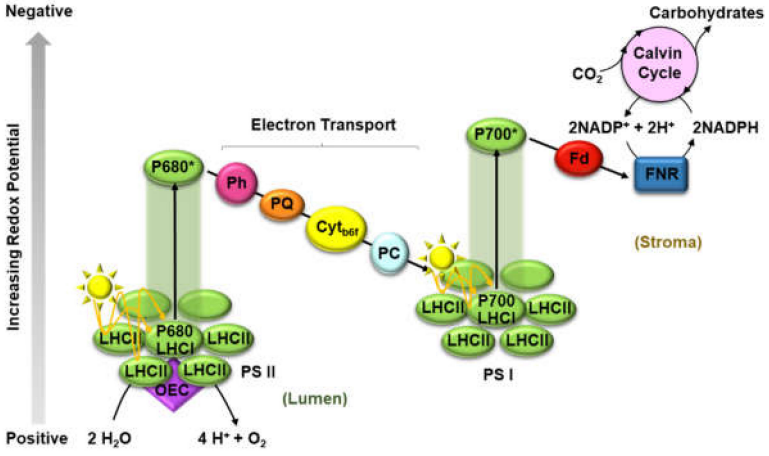

Scheme 1. Simplified Z-scheme of natural photosynthesis.

In this regard, artificial photosynthesis has emerged as a forefront technology to harness solar energy into chemical bonds using available building blocks (CO_2, H_2O and N_2) as feedstock, mimicking natural photosynthesis but at higher efficiencies than natural systems (~1%) [3,13,14]. However, there are a few challenges to address for the fabrication of efficient artificial photosynthetic devices [5,15–17]. First, water oxidation [5,18,19] (WO) and CO_2 reduction [5,20–23] remain bottlenecks. Therefore, advances in mechanistic understanding, comprehension of the factors that control catalytic activity and selectivity [20,24,25], and catalyst development are needed to meet the requirements for practical use: (i) low overpotentials, (ii) high activities, (iii) inexpensive, non-toxic and robust systems [20], and (iv) for CO_2 reduction, specific product selectivity, especially beyond the 2-electron reduction [21,22,26,27]. Secondly, going beyond H_2 and C_1 products (CO, formate) is particularly desirable, since, so far, even with the use of semiconductor materials that are highly efficient in light utilization, only the simplest products derived from CO_2 reduction can be produced. Lastly, charge separation is also pursued to avoid energy losses due to cross-reactivity between the oxidation and reduction sites [17,24,25].

Therefore, the study of molecular systems for their application in artificial photosynthetic devices presents an advantage that is the atom-efficient catalysis with outstanding intrinsic activities and selectivity; as well as their easy tunability and study. However, to this end, important efforts must be directed into the efficient and effective heterogenization of molecular catalysts onto devices. Additionally, long-term stability is very important for the application and stability of the immobilization technique [5,28–31]. This review focuses on the description and general overview of the main strategies used for the heterogeniza-

tion of molecular water oxidation catalysts onto electrodes for (photo)electrochemical water oxidation. Moreover, selected examples for each strategy are explained and compared to their homogeneous counterparts in terms of stability or catalytic activity.

1.2. Water Oxidation Reaction

Water oxidation is the core reaction of natural photosynthesis [32,33] and, as such, it is the central reaction for solar energy conversion and storage [2,3]. However, WO is a highly endergonic process at room temperature and pressure and it still remains one of the bottlenecks for efficient solar-to-fuel conversion due to the harsh oxidizing conditions and high overpotentials required for this transformation [5,34–38]. Development of molecular systems in recent decades has hugely contributed to the field of WO with systems outperforming the activity of the natural system [5,34,35,38,39]. Moreover, the study of molecular water oxidation catalysts has enabled a better understanding of the mechanism of water oxidation catalysis and the extraction of the principles governing catalysis and ligand design [37,39–43]. In this regard, the following considerations should be taken into account for rational design of water oxidation catalysts (WOCs): (i) the multiproton/electron nature of WO, (ii) the synergy between metal centers, (iii) the stabilization effect of the first coordination sphere and the ligand environment, (iv) substrate–catalyst interaction and (v) the thermodynamic stabilization of the protein environment in the O–O bond formation event. Water oxidation is a multistep redox process and, thus, redox-active compounds would be ideal platforms to assist this process by storing oxidizing equivalents and avoiding the formation of highly reactive radical species. In this line, metal oxides and coordination complexes based on transition metals (TM) open a wide range of redox possibilities. In addition, the accumulation of oxidizing power by the TM catalyst can very much benefit from the stepwise proton-coupled electron-transfer (PCET) processes, which lower the thermodynamic energy by avoiding highly charged intermediates. In the case of TM coordination complexes, the ligand environment can play a very important role in stabilizing the different oxidation states at the metal centers. Indeed, basic ligands can stabilize high-valent intermediates due to the significant electron density injection to the metal center. In the same group of stabilizing ligands, we can find anionic or redox non-innocent ligands. Anionic donor ligands constitute good scaffolds to achieve great stabilization of the high oxidation states, but they tend to hydrolyze easily. Further, redox non-innocent ligands have the advantage of facilitating the delocalization of the positive charge of a highly oxidized metal center, to enable the accumulation of oxidizing equivalents. Nevertheless, it is very important to find the right balance between stabilization and reactivity of the active species to prevent an overstabilization that hampers the O–O bond formation.

Catalysts based on biomimetic systems of the oxygen evolving complex (OEC), coordination complexes and organometallic complexes are the most suitable systems for the mechanistic study of water oxidation. These systems have shed some light on the mechanisms for WO and developing efficient and fast catalysts with rates comparable or even higher to that of PSII [35,38,44–46]. One of the most challenging factors in the development and study of those systems is the identification of the exact nature of catalytic activity. The strong oxidizing conditions required for the water oxidation can promote site oxidation reactions on the organic ligand scaffolds, leading to significant structural modifications and hindering further mechanistic investigations. Alternatively, the direct use of inorganic ligands, which are called polyoxometalates, has emerged as a competent possibility in recent years [47]. Polyoxometalates are discrete metal oxides of nanometric size at halfway between molecular complexes and metal oxides [48,49]. Nevertheless, they can also be hydrolyzed under catalytic conditions. Therefore, from a technological point of view, heterogeneous metal oxides have more potential as efficient and robust catalysts for industrial applications since they are more stable under catalytic conditions. Heterogeneous have been developed with the aim to create low-cost, efficient, and more long-lasting WOCs [50–52]. However, it is important to note that regarding mechanistic un-

derstanding, molecular catalysts present lots of advantages such as high catalytic activities, the possibility of rational design and accessible mechanistic investigations.

Among the reported mechanistic studies carried out on the reported systems for WO, two key steps have been identified in the WO reaction: a) the oxidation of the metal center, generating metal-oxo or metal-oxyl (M=O or M-O $^{\cdot}$) reactive species, and b) the O–O bond formation event, which is the rate-determining step (RDS) in most cases. Analogously to the OEC in PSII, two main mechanistic scenarios have been proposed for the O–O bond formation: (i) a water nucleophilic attack (WNA) over a highly electrophilic metal-oxo species (M=O), resulting in a 2e- reduction of the metal center (acid–base mechanism, Scheme 2, left) and (ii) the interaction of two metal-oxyl radical units (M-O·), resulting in a 1e- reduction per metal center (direct coupling (DC), Scheme 2, right). The WNA mechanism is favored with electron-withdrawing ligands, which make the metal-oxo more electrophilic and therefore more susceptible to nucleophilic attack of a water molecule. Moreover, the assistance of an internal or external proton acceptor, binding the water molecule, can facilitate proper orientation to the attack. On the other hand, the DC mechanism is favored by increasing the spin density on the oxygen atoms, generating radical species and facilitating (electronic and sterically) the dimeric interaction [19,34,38,53,54].

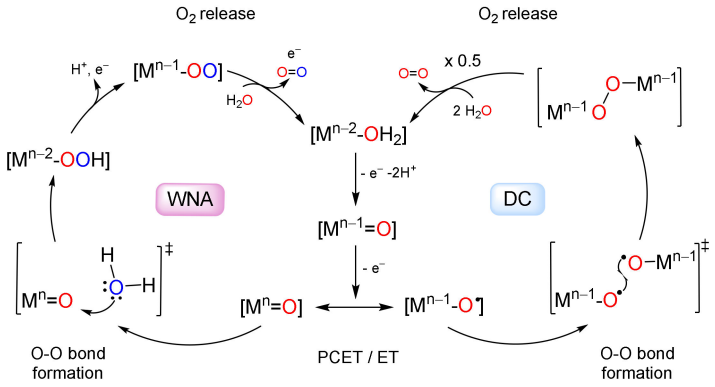

Scheme 2. Summarized main formal mechanistic scenarios for the O–O bond formation in the WO reaction: WNA and DC. $^{\neq}$ Refers to an intermediate transition state structure.

Altogether, since rational ligand and catalysts design toward catalytic activity and durability improvement is crucial to improve catalytic activity and durability, molecular WOCs are highly desirable. The development of highly active and efficient long-lasting WOCs would allow to efficiently couple the WO with reductive transformations (such as CO_2 or water reduction) in artificial photosynthetic devices. Therefore, an alternative approach to the utilization of homogeneous or heterogeneous systems is the immobilization (heterogenization) of molecular water oxidation catalysts (WOCs) together with photoredox catalysts or not on electrodes for (photo)electrochemical WO, which has attracted the interest of the community [28,30,31,55,56].

1.3. (Photo)Electrocatalysts for WO: Homogeneous vs. Heterogeneous and Heterogenization of Molecular Complexes

Molecular catalysts are synthetically versatile and the study of their mechanisms allows rationally modifying and designing ligand scaffolds towards higher activity and stability. Indeed, as we will see in the following lines, the study of molecular-based photoanodes using electrochemistry and their application in electrocatalyzed WO has allowed understanding their mechanism in an efficient manner [57–59], as well as the factors that need to be considered for the development of efficient, robust and highly active systems for their application in artificial photosynthetic devices. However, many catalysts deactivate in (photo)electrocatalytic conditions most likely via bimolecular pathways [30,31,58], diminishing the applicability of the plethora of molecular electrocatalytic systems.

In this context, heterogenization of homogeneous systems by anchoring molecular catalysts on electrode surfaces is a very powerful strategy that combines the high selectivity and activity of molecular systems with the robustness and stability of heterogeneous systems (Table 1) [50,60,61]. Molecular catalysts, however, are far less stable than traditional heterogeneous electrocatalysts, and therefore a method to easily replace anchored molecular catalysts that have degraded could make such electrosynthetic systems more attractive. Moreover, separation of the active centers upon immobilization onto electrodes also disfavors bimolecular decomposition pathways.

Table 1. Comparison of properties of homogeneous, heterogeneous and heterogenized catalysts.

Property	Homogeneous	Heterogenous	Heterogenized
Activity	High	Moderate	High
Selectivity	High	Low-Medium	High
Synthesis	Complex	Simple	Complex
Tuneability	High	Low	High
Efficiency	Moderate	High	High
Stability	Short term	Long-term	Elongated
Robustness	Low	High	High
Study	Established protocols, valuable information	Less explored	Established protocols, valuable information

2. Approaches for the Development of WO (Photo)Anodes

Heterogenization of homogeneous systems by anchoring molecular catalysts on electrode surfaces is a very powerful strategy that combines the advantages of both homogeneous and heterogeneous systems. Therefore, these systems possess the high selectivity and activity of molecular systems with the robustness and stability of heterogeneous catalysts [28,30,31,55,60]. Moreover, surface-bound catalysts for electrocatalytic WO allow for easier recovery of the catalysts and the use of a wider variety of solvents due to the suppression of solubility issues in the bulk solution.

The most widespread anchoring strategies for the immobilization of molecular WOCs onto (photo)electrodes differ on the type of interaction used for the WOC immobilization, which can be covalent or non-covalent [30,31,55]. The choice of immobilization strategy depends on the type of electrode material and the tolerance of the molecular catalysts. Common immobilization strategies are summarized below (Figure 1):

- Covalent anchoring,
- Supramolecular interactions,
- Drop-casting,
- Physical confinement into porous materials such as metal organic frameworks (MOFs) or covalent organic frameworks (COFs),
- Electropolymerization,
- Atomic layer deposition (ALD), and
- Layer-by-layer deposition.

2.1. Covalent Immobilization

Immobilization of molecular WOCs by ligand modification that allows further covalent functionalization of (photo)electrodes is the most extensively studied approach [30,55]. Despite the fact that the most common strategy involves the modification of the ligand backbone of the molecular WOCs for their subsequent attachment to the surface of the photoelectrode [62], depending on the type of WOC, semiconductor, metal oxide or conductive glass of the (photo)electrode, different strategies can be employed. For the covalent functionalization of the ligand backbones with surface anchoring groups, a similar approach to the one used in the design of light-harvesting dyes for dye-sensitized solar cells (DSSC) is followed [63,64]. Among the most common functional groups that allow further surface covalent anchoring by click chemistry, the carboxylate [65,66], phosphate [67–69],

hydroxamate, and hydroxyl [70,71] functional groups (Figure 1a) can be immobilized onto a photoelectrode by an esterification reaction with its surface. This strategy has been used for the immobilization of several WOCs [72–77] on oxide semiconductors (see Section 3.1 for further selected examples) [62,65,72,78,79].

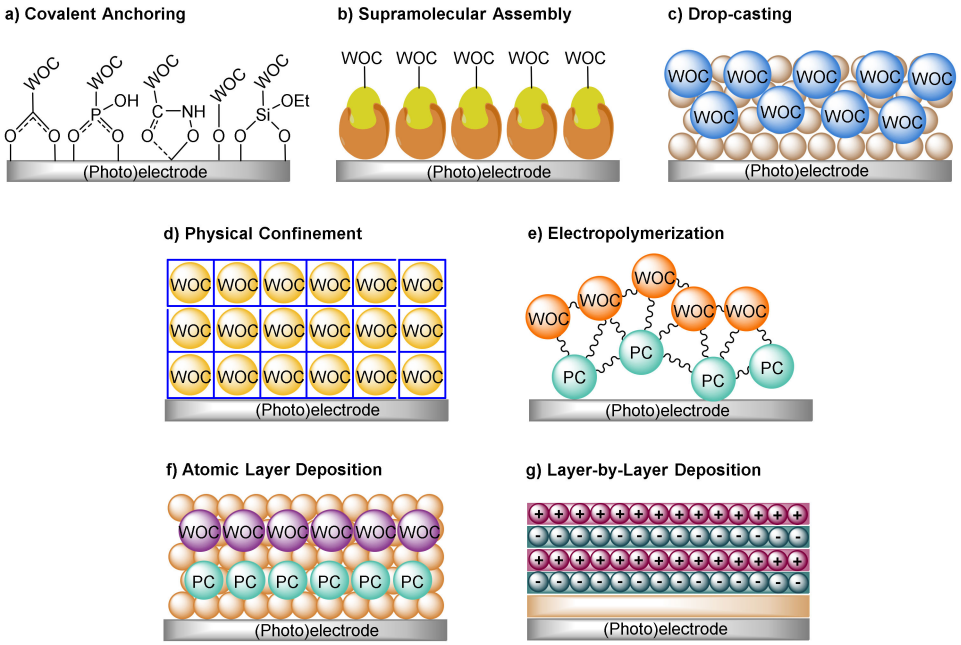

Figure 1. Summarized strategies for the heterogenization of molecular water oxidation catalysts on (photo)electrodes: (**a**) covalent functionalization, (**b**) self-assembly and other supramolecular interactions, (**c**) drop-casting immobilization, (**d**) physical confinement in porous materials such as MOFs/COFs, (**e**) electropolymerization, (**f**) atomic layer deposition (ALD), and (**g**) layer-by-layer deposition.

However, a decrease in catalytic activity is a common feature when this immobilization strategy is used, which can be attributed to changes in the electronic and energetic effects in the catalyst upon the introduction of anchoring functional groups to the ligand of the WOCs that modify their redox potentials and catalytic activity and also catalyst stability [30,62,80–82]; or the hydrolytic degradation of ester linkages in both acidic or basic conditions [62], resulting in detachment of the molecular catalysts from (photo)electrodes [5,62,80].

Therefore, to address these issues, several alternatives have been used. On the one hand, functional groups that are used as anchors have been introduced further from the active side by using long alkyl chains as spacers in the linkers [75,83,84]. This approach causes fewer electronic changes in the active side of WOCs as well as minimizes direct interactions with the (photo)electrode surface, preserving their catalytic activity and minimizing electron-hole recombination, respectively. Additionally, more chemically and thermally stable anchoring groups or multiple anchoring groups have been employed such as pyridine-2,6-bicarboxylic acid [76], 1-(3′-amino)-propylsilatrane [85], and pyridine-N-oxide 2-carboxylic acid [86], among others [63,77], at the expense of complex synthetic procedures and charge recombination at the WOC/(photo)electrode/electrolyte interfaces [39,62]. Alternatively, phosphonate surface binding sites that are more stable in acidic conditions, or metal-oxo bridging sites, have also been used as linkers, since they are more stable than ester groups [87].

An alternative approach to avoid changing the properties of the molecular WOCs is the modification of the surface of the (photo)electrodes for subsequent covalent attachment of the WOC [55,88–90]. In this regard, alkoxysilanes with specific end-functional groups (such as amines or pyridine derivatives) have been widely used for surface modifi-

cation of several (photo)electrodes, such as TiO_2 [64,89,91,92], ZnO [93–95], and SnO_2 [96], due to their simple functionalization surface chemistry [88,90]. For instance, with the 3-aminoproyltriethoxysilane (APTES) moiety, amine groups can be readily displayed on photoelectrode surfaces by hydrolytic condensation, where WOCs can be immobilized at a later stage.

2.2. Supramolecular Host–Guest Interactions

This approach uses supramolecular chemistry to assemble WOCs into guests-electrode moieties forming large functional structures by self-assembly processes, offering a toolbox to develop WO (photo)anodes. Moreover, for WOCs that operate following a dinucelar mechanism (DC) to form the O–O bond, this strategy can enhance the reaction rate by approaching the two metal-oxo units or increasing the local concentration of active species due to the host–guest interactions [97,98], as has been previously observed for ligand systems that favor Π-Π-stacking interactions between two metal complexes [44,99], by self-assembly into micelles [100], or by encapsulation into mesoporous guests [101] or macrocycles [102].

In this context, most common methods rely on Π-Π-stacking, hydrogen bonding or coulombic interactions for the assembly of WOCs onto a guest that is deposited onto an electrode or directly functionalized on its surface. Alternatively, when the (photo)electrodes are hydrophobic, WOCs bearing hydrophobic polyaromatic functional groups can also be utilized as a surface anchoring group via hydrophobic interactions directly onto the electrode [30,55,103]. However, this latter approach would have limited stability, since these hydrophobic interactions are vulnerable to aggregation or disassembly in aqueous solutions under catalytic conditions [104,105].

Another advantage of this immobilization strategy is that, since the catalyst is generally immobilized onto a guest that is anchored on the electrode, there are fewer problems of charge recombination and it can also help stabilize reactive intermediates within the guest via supramolecular interactions [30,31,55,60,97,103].

2.3. Drop Casting

This is an immobilization strategy that consists of the physisorption of a solution of a WOC onto the (photo)electrode surface followed by evaporation of the solvent without requiring the introduction of functional groups in the molecular WOC to enable its anchoring. The disadvantage of this approach is that it is difficult to control the film thickness and achieve a uniform coating, so it can reproducibility issues may arise [106]. Moreover, it normally requires the coaddition of binders, such as Nafion [107], to facilitate the anchoring of the catalyst, which is costly and can hamper its applicability [108–110].

2.4. Immobilization via Physical Confinement

Another immobilization strategy that is very appealing to increase the density of active sites onto electrodes is via physical confinement of WOCs into porous hosts materials such as MOFs or COFs. This approach has the advantage of avoiding complex and tedious ligand modification or functionalization processes and thus, also avoiding changes in the inherent electrochemical and energetic parameters of the catalysts. This strategy allows for simple immobilization of molecular WOCs with or without other co-catalysts or photoredox catalysts in porous materials [111]. Another advantage is the host matrices can have their own functionality that complements the WOC, such as light harvesting, charge separation, passivation and stabilizing coating layers for the whole assembled (photo)anode. [111]

For this approach, the immobilization of catalysts in the host material can be achieved following three methods: (i) by mixing a preformed host material with a presynthesized WOC and allowing the impregnation of the catalyst onto the material; by (ii) a bottom-up assembly of a host material around the preformed WOC; and (iii) using an hybrid alternative that combines both methods [112].

Despite this method being suitable for avoiding tedious synthetic procedures and allows confinement of the catalysts in the material with negligible change in its properties, one challenge of this strategy is the choice of the host material pore size. On the one hand, the pore size of the host materials should be larger than the size of molecular WOCs, although this can lead to catalyst leaching from the host material and a decrease in catalytic activity. On the contrary, if the pores are similar in size to the WOC, blocking of the host material porous upon immobilization can also limit catalytic activity [30,55].

Among possible porous hosts materials, metal–organic frameworks (MOFs) have gained great attention due to their interesting properties originating from their flexibility in structure and synthetic methods, allowing a large degree of structural and chemical tunability [30,55,111,113–115].

2.5. Electrografting/Electropolymerization

This strategy is based on the immobilization of molecular electrocatalysts by in situ hybridization with functional groups that can undergo polymerization under applied potential on the surface of photoelectrodes. In this regard, following this strategy, molecular WOCs can be either electro-polymerized or -oligomerized themselves or, alternatively, molecular WOCs can be incorporated in situ during electropolymerization of conductive matrix polymers on the desired photoelectrode. This strategy enables the preparation of photoelectrodes for WO with long photostability and catalytic activity without significantly altering the physical and electrochemical properties of the immobilized catalysts within the polymer films. Therefore, this approach enables the screening of several catalysts onto (photo)electrodes. Moreover, with these methods, catalysts are deposited forming a uniform polymeric film, the thickness of which can be controlled [30,31,55]. This approach has been used for the multicomponent assembly of dyes and catalysts on metal oxide electrodes for applications in dye-sensitized photoelectrochemical cells (DSPECs) [116].

In this context, electrografting is commonly used for the functionalization of carbon-based electrodes since they are inexpensive and can be straightforwardly modified [117,118]. In this case, diazonium electrografting is used to attach molecular catalysts onto carbon electrodes forming covalent bonds [118].

2.6. Atomic Layer Deposition

This is a relatively new strategy for preparing spatially controlled, multicomponent films consisting of molecular light-absorbing chromophores and water oxidation catalysts on high-surface-area porous metal oxides. It was initially developed by Templeton and Meyer to prepare (photo)anodes in a more efficient manner and render more stable hybrids [119]. This approach consists of depositing a thin layer of inert aluminum oxide (Al_2O_3) onto the surface of a dye that is surface bound to an electrode, covering it, and followed by catalyst (WOC) binding to the new oxide surface. In a final step, catalyst surface binding is stabilized by a another ALD overlayer of Al_2O_3. The ALD assembly procedure bypasses synthetic difficulties arising from the preparation of phosphonic acid-derivatized, covalently linked assemblies.

2.7. Layer-by-Layer Assembly: Electrostatic Self-Assembly Non-Covalent Immobilization

The layer-by-layer (LbL) deposition strategy is a thin-film fabrication technique based on the alternate deposition of layers of oppositely charged species that was initially developed by J. J. Kirkland of DuPont [120]. Therefore, the polyelectrolyte self-assembly occurs by the alternate exposure of an electrode surface to solutions of oppositely charged polyelectrolytes or polyions [121,122]. Finally, electrostatic, non-covalent immobilization strategies can be employed for the immobilization of molecular electrocatalysts. Moreover, this strategy can be combined with other immobilization techniques or set ups for several applications and thus has been used for the fabrication of diverse functional hybrid materials for a manifold of applications in biomedicine, energy conversion and storage and catalysis [121–123]. Additionally, an advantage of LbL is that it is a general strategy

that can be applied to any (photo)electrode surface regardless of their type of material and shape [122–125].

3. Selected Examples of WO (Photo)Anodes

In this section, selected examples of molecular catalysts immobilized onto (photo)electrodes using different strategies explained above are revised and the respective advantages of their molecular counterpart analyzed. In most reported systems, molecular WOCs are immobilized on semiconductors and metal oxides. Additionally, the coimmobilization of dyes together with molecular WOCs or molecular dyads or triads containing WOCs, photosensitizers and electron mediators enables light-driven photoelectrocatalyzed WO. These assemblies can be applied in artificial photosynthetic devices.

3.1. Covalent Anchoring of Molecular WOCs onto Electrodes

This strategy is very versatile since many groups can be incorporated to the ligand scaffolds of molecular WOCs to covalently anchor them to (photo)electrode surfaces [55,57,62]. Several molecular WOCs based on Ru, Fe, Co, Mn, Fe and Cu have been explored for (photo)electrochemical WO using this immobilization strategy onto electrode surfaces [39,43,56,60–62,126,127].

Among all examples, Li et al. reported a molecular Ir WOC covalently bonded to hematite photoanodes in a monolayer using an oxobridge between the Ir active sites and the Fe element of the photoanodes (Ir-O-Fe) forming a ultra-thin film with greatly increased photocatalytic activity for WO at acidic pH (WOC-1, Figure 2a), which was remarkable taking into account that there are still only a few heterogeneous OER electrocatalysts that maintain high catalytic activity and stability at acidic pH values, such as highly expensive IrO_x [128]. This heterogenized Ir-WOC exhibited much higher activity than its homogeneous counterpart and was active within a water-splitting device with stable activity for over 5 h at near 100% FE at acidic pH, which was the first example reported to complete unassisted water splitting by hematite-derived electrodes in acidic solutions. This was associated with the efficient transfer of charge carriers between the photoelectrode and the catalyst. However, the system needed further work to stabilize the WOC/hematite combination. At the same time, Hintermair, Crabtree and Brudvig reported the immobilization of the same system on metal oxides showing increased catalytic activity and stability [129]. The system was reported to produce over 100,000 TON O_2 per iridium atom after ~16 h of electrolysis, and XPS studies confirmed the stability of the system.

Another example using covalent immobilization of WOCs onto electrode surfaces was reported by the group of Sun. They reported a Ru-WOC-bearing 2,6-pyridinedicarboxylic acid (PDC) ligand that could be efficiently immobilized on hematite nanorod arrays via the carboxylic acid groups together with a Ru photoredox catalyst anchored via phosphonate functional groups $[Ru(4,4'\text{-}(PO_3H_2)_2\text{-bpy})(bpy)_2]^{2+}$ (4,4′-$(PO_3H_2)_2$-bpy = [2,2′-bipyridine]-4,4′-diylbis(phosphonic acid) and bpy = 2,2′-bipyridine) (WOC-2 and PC-1, respectively, Figure 2b). The system showed efficient solar WO at alkaline pHs with a steady photocurrent of 25 μA cm^{-2} [76]. Moreover, the photoanode was stable at various pHs for a prolonged time for over 3 h due to the employment of strong PDC anchoring group. Using the same carboxylic acid as anchoring groups, L-Z. Wu et al. reported the immobilization of a Co-WOC bearing a porphyrin with carboxyl groups, CoTCPP (TCPP = meso-tetra(4-carboxyphenyl)porphyrin) on Al_2O_3-modified BiVO4 photoanodes for PEC water oxidation [130]. Under illumination of a 100 mW cm^{-2} Xe lamp, the photoanode exhibited a 2-fold enhancement in photocurrent density at 1.23 V vs. RHE and nearly a 450 mV cathodic shift at 0.5 mA cm^{-2} photocurrent density relative to bare $BiVO_4$ at pH = 6.8 in a PEC configuration, generating O_2 and H_2 with a faradic efficiency of 80% over 4 h. Moreover, the authors demonstrated that immobilized molecular CoTCPP catalyst greatly suppressed the hole–electron recombination on the surface of $BiVO_4$ semiconductor. Besides organometallic compounds, these approaches are also effective for the assembly and integration of other molecular catalysts [76,107,131].

Then, using silane-prefunctionalized electrodes and the same $[Ru(4,4'\text{-}(PO_3H_2)_2\text{-}bpy)(bpy)_2]^{2+}$ as photoredox catalyst, the group of Sun reported a FTO/TiO_2 photoanode bearing the Ru photocatalyst immobilized via the phosphonate anchoring and a Ru-bda [132] derivative Ru-WOC [Ru(bda)(pic)(L)] (L = *N*-(3-(triethoxysilyl)propyl)isonicotinamide) anchored by the silane groups (PC-1 and WOC-3 Figure 2c) [91]. This system was active for visible light-driven water splitting at pH 6.8 evolving O_2 and H_2 at 0.2 V vs. NHE applied, generating a high photocurrent density > 1.7 mA cm^{-2} after 10 s light irradiaiton, which at that time was higher than any PEC devices with molecular components reported in the literature. Other systems have been reported using silanes as anchoring groups in Ru-bda derivative WOCs by Meyer and coworkers showing high activity for photoelectrocatalyzed WO, but the system showed long-term loss of catalytic activity due to catalyst loss from the electrode surface by axial ligand dissociation in the high oxidation states of the WOC [96].

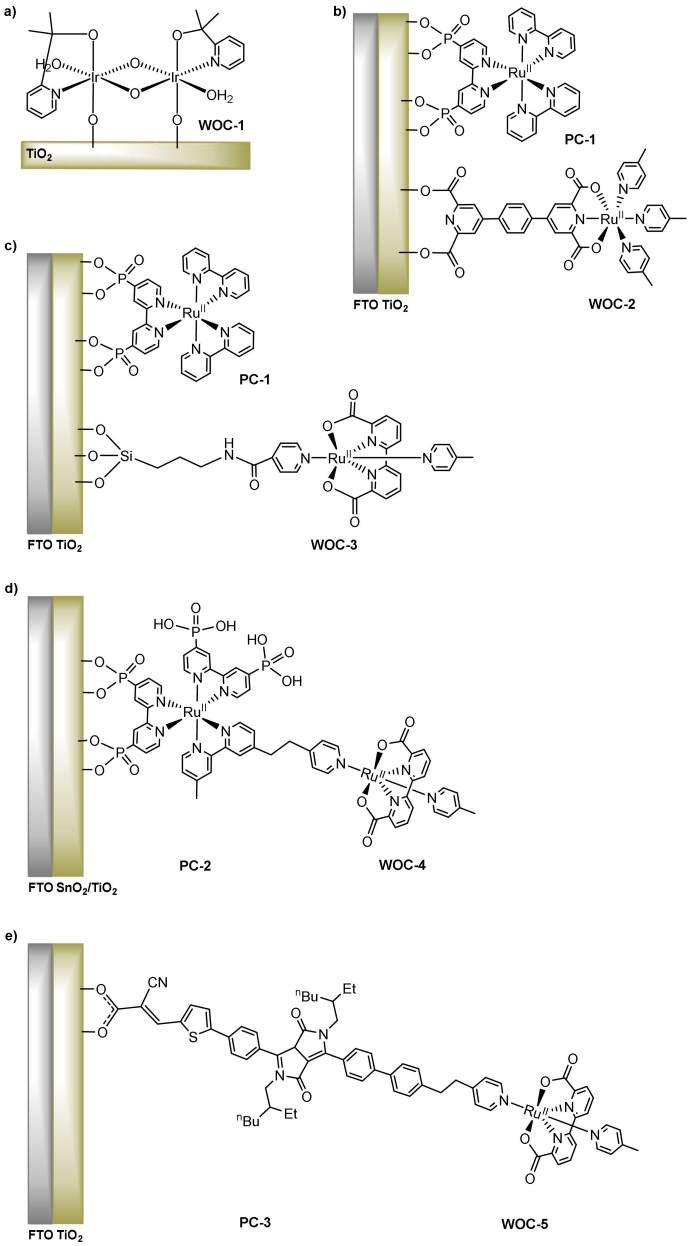

Figure 2. Selected examples of covalently immobilized WOCs onto (photo)electrodes. (**a**) Ir-WOC oxo-bridged photoanode [128], (**b**) $[Ru(4,4'\text{-}(PO_3H_2)_2\text{-}bpy)(bpy)_2]^{2+}$ and Ru(PDC)(pyridine) [76], (**c**) $[Ru(4,4'\text{-}(PO_3H_2)_2\text{-}bpy)(bpy)_2]^{2+}$ and Ru(bda)(pic)(Het) [91], (**d**) $[Ru(4,4'\text{-}(PO_3H_2)_2\text{-}bpy)(bpy)_2]^{2+}$ and $[Ru(bda)Het_2]$ [133], and (**e**) DPP-Ru-WOC dyad system [73].

Meyer and Concepcion reported a new Ru-based polypyridylbased chromophore−catalyst assemblies, [Ru(4,4′-$(PO_3H_2)_2$-bpy)$_2$(4-Mebpy-4′-epic)-Ru(bda)(pic)]$^{2+}$ (Mebpy-4′-epic = 4-(4-methylbipyridin-4′-yl-ethyl)-pyridine; bda = 2,2′-bipyridine-6,6′-dicarboxylate; pic = 4-picoline, PC-2 and WOC-4, respectively, Figure 2d) covalently anchored on a SnO_2/TiO_2 core shell electrode to be applied in a dye-sensitized photoelectrosynthesis cell (DSPEC) for solar water splitting with a Pt cathode. This was the first reported covalently linked chromophore–catalyst assembly incorporating a Ru-bda-derived WOC that performed both electrochemical and photoelectrochemical WO on oxide surfaces. The system was active for light-driven WO at pH 5.7 and under white illumination (100 mW cm^{-2}) photocurrents of 0.85 mA cm^{-2} were observed after 30 s under a 0.1 V vs. Ag/AgCl applied bias with a FE for O_2 production of 74% after 5 min irradiation [133]. The same group then reported the use of the same phosphate anchoring group to immobilize a Ru photoredox catalyst [Ru(4,4′-$(PO_3H_2)_2$-bpy)(bpy)$_2$]$^{2+}$ (4,4′-$(PO_3H_2)_2$-bpy = [2,2′-bipyridine]-4,4′-diylbis(phosphonic acid) and bpy = 2,2′-bipyridine) and a derived Ru-bda [Ru(bda)Het$_2$] [133] (bda = 2,2′-bipyridine-6,6′-dicarboxylate) WOC with phosphonate anchoring groups onto MO_x/FTO electrodes to develop a photoanode for use in a DSPEC [75]. The system was active for photoelectrocatalyzed WO, generating a photocurrent of 1.4 mA cm^{-2} at pH 7 with minimal loss of catalytic activity over 30 min, with an IPCE of 24.8% at 440 nm.

Another approach was reported by Reisner and coworkers, where they developed a dyad photocatalyst consisting of a diketopyrrolopyrrole chromophore (DPPdye, PC-3, Figure 2e) and Ru-based WOC (WOC-5) featuring a cyanoacrylic acid anchoring group for its immobilization onto a mesoporous TiO_2-derived FTO/TiO_2 electrode. The assembled dyad-sensitized photoanode was active for O_2 evolution using visible light (100 mW cm^{-2}, AM 1.5G, $\lambda > 420$ nm), producing a initial photocurrent of 140 mA cm^{-2} at pH 5.6 under an applied potential of 0.2 V vs. NHE, with 44% FE with a TON of 2.3 for the WOC and 9.2 regarding the dye [73]. Under photoelectrochemical experiments, the photocurrent decreased during irradiation time, which was associated with catalyst detachment or decomposition, whilst the dyad remained adsorbed onto the electrode and the chromophore was intact.

3.2. Supramolecular Assembly of Molecular WOCs onto Electrodes

This strategy has gathered interest since it allows reversible immobilization of the WOCs onto guests that are anchored in the electrodes. One advantage of this approach is that it allows the detachment of the deployed WOC from the guest-electrode surface once catalytic activity decreases, as well as reattachment of a new batch of fresh catalyst to restart catalytic activity. Moreover, as seen in the previous section, this strategy generally avoids significant changes in the electrochemical and energetic properties of the WOCs [30,31,55,60,97,103].

In this line, the group of Reek mention a supramolecular encapsulation strategy to immobilize ruthenium complexes onto electrodes. Their approach involved the use of $M_{12}L_{24}$ nanospheres [134] (where M correspond to the corners which are Pt^{2+} or Pd^{2+}, and L the bipyridyl building block) endohedrally functionalized with guanidinium that can strongly bind to other sulfonate bearing-catalysts via hydrogen bonding interactions. Therefore, they developed two Ru complexes derived from the [Ru(bda)Het$_2$] [132] WOC (bda = 2,2′-bipyridine-6,6′-dicarboxylate) and [Ru(phenda)(Het$_2$)] (phenda = [1,10] phenanthroline-2,9-dicarboxylic acid) [135] bearing sulfonate functionalized pyridine axial ligands for supramolecular attachment to the guanidinium nanospheres: [Ru(bda)($PySO_3TBA)_2$] and [Ru(phenda)($PySO_3TBA)_2$] based on the $PySO_3TBA$ = pyridine-3-sulfonate, WOC-6 and WOC-7, respectively, Figure 3a). The encapsulation of dilute solutions of the catalysts (10^{-5} M) inside the guests lead to high local catalyst concentrations (up to 0.54 M). In the case of WOC-6, the increase in local concentration resulted in an enhanced water oxidation rate by two-orders of magnitude to 125 s^{-1}, 130-fold higher than that observed for the non-encapsulated catalyst [98]. This was attributed to a facilitated diffusion-controlled

rate-limiting dinuclear coupling step, since for complex WOC-6 a dinuclear DC mechanism (radical oxo coupling) to form the O–O bond is also possible [53]. While for WOC-7, since it exclusively operates via WNA [135], the reaction rate for WO did not change by encapsulation of the catalyst. Electrolysis experiments at 1.3 V showed 3-fold more current that in the absence of nanosphere for WOC-6 with 96.3% Faradaic efficiency for O_2 solution using a rotating disk electrode. This example showed that great rate enhancements can be achieved by spatial organization of catalytically active species following the dinuclear mechanism [98]. Moreover, this strategy was proven successful to modulate reaction rates by changing local catalyst concentrations by supramolecular interactions and it enabled the study of electrocatalytic reaction mechanisms.

Another strategy was reported by Sun and coworkers, where they used supramolecular interactions to assemble a DSPEC for water splitting using poly(methylmethacrylate) (PMMA) as auxiliary binder and stabilizing material [136,137] and a Ru-WOC modified with long hydrocarbon chains via hydrophobic interactions. They used a phosphonate functionalized Ru-photoredox catalyst $[Ru(4,4'\text{-}(PO_3H_2)_2\text{-}bpy)(bpy)_2]^{2+}$ (4,4′-$(PO_3H_2)_2$-bpy = [2,2′-bipyridine]-4,4′-diylbis(phosphonic acid) and bpy = 2,2′-bipyridine) and heterogenized it on a TiO_2/FTO electrode by the phosphate anchoring groups, and a Ru-bda [132] derivative WOC [Ru(bda)(pic)(Het)] (bda = 2,2′-bipyridine-6,6′-dicarboxylate, pic = 4-picoline) with one of the axial pyridine ligands modified with a C_{12} hydrophobic alkyl chain, which was mixed with PMMA in solution and co-assembled with the dye-TiO_2/FTO electrode to generate the WO photoanode. The aliphatic chain was crucial to obtain stable light-driven water oxidation catalysis keeping the catalyst in the polymer matrix [138]. Upon irradiation, the photoanode generated a photocurrent density of 1.1 mA cm^{-2} and an incident-photocurrent conversion efficiency (IPCE) of 9.5% at 0.2 V vs. NHE applied bias. Moreover, the catalytic system displayed good stability during photocatalytic experiments. Later, the group of Concepcion used a similar Ru-WOC functionalized with a C_{10} alkyl chain in one of the axial pyridines [Ru(bda)(pic)(4-C10H21-py)] (WOC-8, Figure 3b) and combined it with an aliphatic C_9 chain functionalized Ru-based photoredox catalyst $[Ru(4,4'\text{-}(PO_3H_2)_2\text{-}bpy)_2(4,4'\text{-}(C_9H1_9)_2\text{-}bpy)]^{2+}$ (PC-4, 4,4′-$(PO_3H_2)_2$-bpy = [2,2′-bipyridine]-4,4′-diylbis(phosphonic acid) and bpy = 2,2′-bipyridine) that also had phosphonate functional groups to allow anchoring onto electrode surfaces, preparing therefore, supramolecular assemblies of Ru-WOC and Ru dye in the hydrophobic interface and immobilized onto metal oxide-based electrodes. Moreover, in the same report, they also showed the functionalization of metal oxide electrode surfaces with self-assembled monolayers with long hydrophobic chains, which enabled the supramolecular immobilization of Ru-WOCs also functionalized with long alkyl chains, rendering more stable electrodes [103]. A follow-up paper of the same group used their previously reported WOC-8 and PC-4 assembly prepared by a self-assembled bilayer on a mesoporous SnO_2/TiO_2 core/shell electrode (FTO | SnO_2/TiO_2 | PC4-WOC-8, Figure 3b). This photoanode was highly active for WO for over 3 h with 86% FE for O_2 production. Under 1 sun illumination, the photoanode reached a photocurrent density of 2.2 mA cm^{-2} with an IPCE of 29% at 450 nm [139]. This demonstrated that hydrophobic interactions are suitable to in situ assemble and catalysts and chromophores on electrode surfaces.

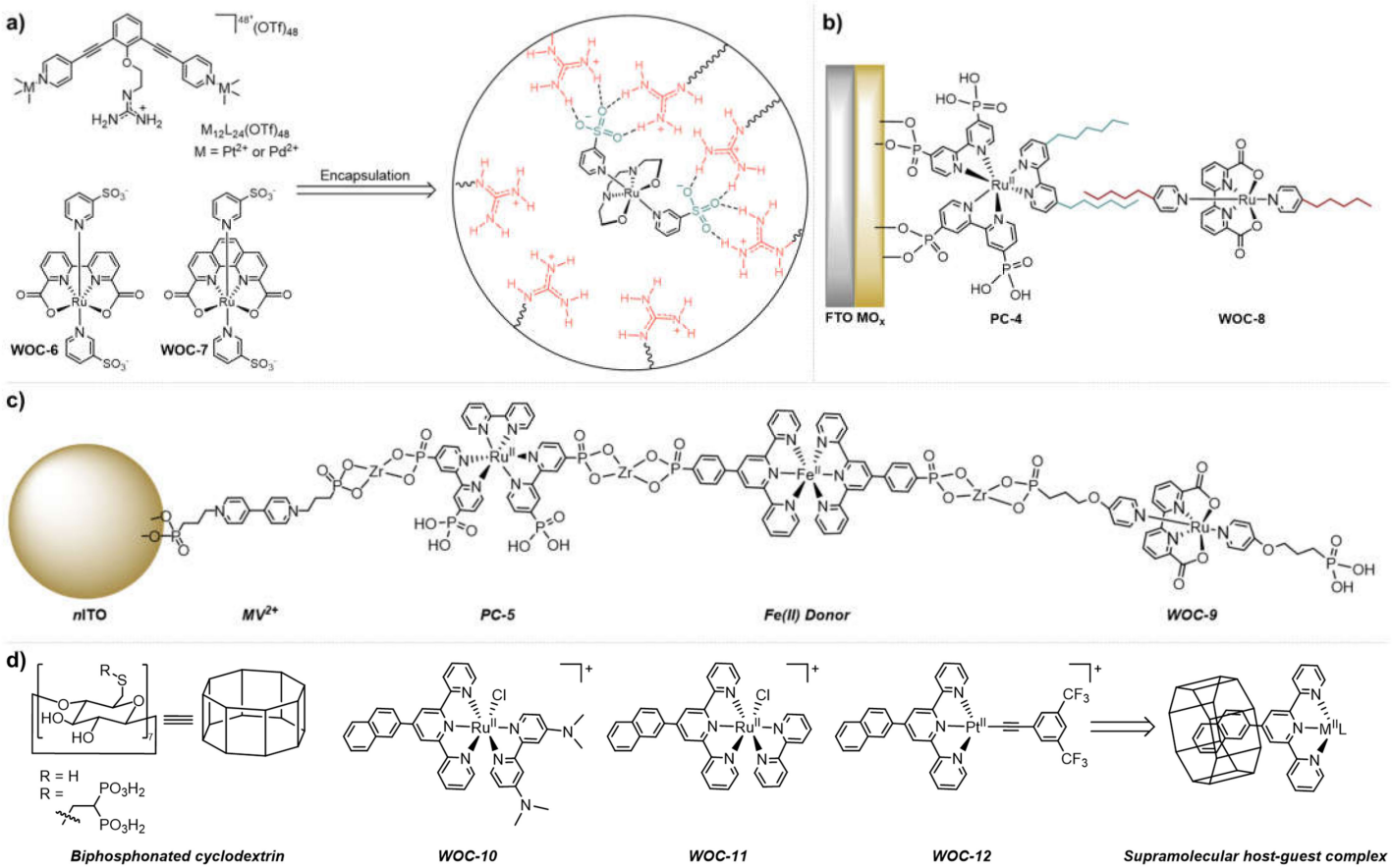

Figure 3. Selected examples of supramolecular assemblies for (photo)electrochemical heterogenized water oxidation. (**a**) assembly of [Ru(bda)($PySO_3TBA)_2$] and [Ru(phenda)($PySO_3TBA)_2$] complexes in guanidinium functionalized nanospheres [98], (**b**) [Ru(4,4′-$(PO_3H_2)_2$-bpy)$_2$(4,4′-$(C_9H_{19})_2$-bpy)]$^{2+}$ and [Ru(bda)(pic)(4-$C_{10}H_{21}$-py)] assembled onto a metal oxide-based electrode [103,139], (**c**) multicomponent assembly of MV^{2+}, [Ru(bpy)(4,4′-$(PO_3H_2)_2$-bpy)$_2$]$(Cl)_2$, [Fe(2,2′:6′,2′′-terpyridyl-4-phenyl-phosphonic acid)]$(Cl)_2$) donor and [Ru(bda)((3-(pyridine-4-yloxy)propyl)phosphonic acid)$_2$ [72], and (**d**) bioinspired cyclodextrin and tpy derivative Ru and a Pt WOCs and simplified formation of the host–guest complex [140].

Then, using a similar Ru WOC ([Ru(bda)((3-(pyridine-4-yloxy)propyl)phosphonic acid)$_2$], WOC-9) and photoredox catalyst ([Ru(bpy)(4,4′-(PO_3H_2)$_2$-bpy)$_2$]$(Cl)_2$, PC-5, Figure 3c), and inspired by the supramolecular Zr-phosphonate chemistry developed by the group of Mallouk and used to prepare dye–catalyst assemblies using a layer-by-layer [141], the group of Meyer used this strategy to construct a preorganized multicomponent assembly consisting of electron acceptors, electron donors, photoredox catalysts and WOCs (MV^{2+} (methyl viologen), PC-5, Fe(II) donor ([Fe(2,2′:6′,2′′-terpyridyl-4-phenyl-phosphonic acid)]$(Cl)_2$) and WOC-9, respectively, see Figure 3c), with the attempt to prepare a bioinspired artificial analogue of PSII [72]. The location of the components on the electrode also mimics the spatial arrangement of the key elements of PSII: conducting oxide electrode surface (Plastoquinone in PSII), MV^{2+} (pheophytin), PC-5 (P680 Dimer), Fe(II) donor (tyrosine) and WOC-9 (Mn cluster of the OEC), generating a *nano*ITO|-MV^{2+} -PC-5 -Fe(II)donor -WOC-9 photoelectrode assembly. In a three-electrode configuration photoelectrochemical cell, under 1 sun illumination (100 mW cm^{-2}, 400 nm filter cut off) for 30 s at pH 4.65 a photocurrent density of 250 μA cm^{-2} were generated at 0.5 V vs. NHE applied bias. In continuous O_2 evolution experiments, the photocurrent decreased to 75 μA cm^{-2} after the first 10 min of reaction and remained constant at 50 μA cm^{-2} for over 1 h of irradiation with a FE for O_2 production of 67%. Further studies demonstrated that the system generated reductive equivalents at the electrode surface and oxidative equivalents at the WOC side a catalyst that persist for seconds in aqueous solutions, proving the ability of the system to mimic functional elements of PSII including charge separation and water oxidation. Moreover, steady-state illumination of the assembly with 440 nm light with an applied bias results in photoelectrochemical water oxidation with a per-photon absorbed efficiency of 2.3% after 10 s of photolysis [72].

More recently, the same group reported a related study describing a single molecular assembly electrode that duplicated the key components of PSII, consisting of a dyad formed by a similar Ru phosphonated polypyridyl photoredox catalyst, supramolecularly linked to an intermediate electron donor via the supramolecular Zr-phosphonate chemistry, and covalently linked to a molecular-based Ru-bda-derived WOC and protected and stabilized by a 4,5-difluoro-2,2-bis(trifluoromethyl)1,3-dioxole (AF) polymer on a SnO_2/TiO_2 core/shell electrode. This photoanode mimicked PSII in achieving sustained, light-driven WO catalysis. Under illumination and at pH 7 the photoanode produced O_2 with an efficiency of 83% and an IPCE value of 10.9% at its absorption maximum of 460 nm, with an applied bias of 0.6 V vs. NHE. This example highlighted the value of the tyrosine–histidine pair in PSII in achieving efficient water oxidation catalysis in artificial photosynthetic devices by the introduction of the intermediate electron donor between the photoredox catalyst and the WOC [142].

Using hydrophobic interactions as a strategy to incorporate Ru WOCs onto electrode surfaces to perform electrocatalyzed WO at neutral pH, Llobet and coworkers reported oligomeric Ru complexes that can be simply anchored on the surface of multiwalled carbon nanotubes via CH–Π interactions between the axial ligands bound to the Ru-WOCs and the hexagonal rings of the graphitic surface of the material, providing control of their molecular coverage. These hybrid molecular materials behaved as molecular anodes that catalyzed WO at pH 7 with high current densities [143]. With the same immobilization strategy, the same group reported a homogeneous Cu-WOC featuring a tetraanionic amidate ligand N_1,N_1′-(1,2-phenylene)bis(N_2-methyloxalamide) was derivatized with a pyrene moiety in the pyridine ligand were supported onto graphite electrodes through supramolecular Π-Π-stacking supramolecular interactions. This system showed electrocatalyzed WO activity at 538 mV vs. NHE overpotential, which was 160 mV lower than its homogeneous counterpart, and higher rate (540 s^{-1}). This enhancement of catalytic activity was attributed to the pyrene moiety and the electrode stacking interactions [144]. Additionally, Co-corrole complexes have also been immobilized for electrocatalyzed water splitting using the same immobilization strategy [145].

Finally, the group of Tilley applied a non-covalent chemistry approach to reversibly bind molecular electrocatalysts to electrode surfaces through host–guest complexation with surface-anchored bioinspired cyclodextrins, since allows for strong binding between the host and the guest and enables the flow of electrons between the electrode and the guest catalyst. The authors reported the use of two different molecular Ru and a Pt WOCs bearing a naphthalene moiety as substituent in the 2,2′:6′,2′′-terpyridine derivative ligand to allow assembly with the host: WOC-10, WOC-11 and WOC 12, respectively (Figure 3d). These systems showed a greater stability when immobilized onto the electrode surface than in solution, which was attributed to the large binding energies obtained by DFT calculations. Electrosynthesis in both organic and aqueous media was demonstrated on metal oxide electrodes, with stability on the order of hours. Moreover, the authors showed that the catalytic surfaces could be recycled by controlled release of the guest from the host cavities and the reabsorption of fresh WOC guest by tunning the conditions [140]. This study showed the suitability of multidentate supramolecular hosts as the anchoring moieties for molecular WOC guests to generate stable and electrocatalytically active surface-bound host–guest complexes in both aqueous and organic solvents for electrocatalytic WO.

3.3. Integration of Molecular WOCs onto Electrode Surfaces by Drop-Casting

The group of Sun reported the immobilization of a molecular Co_4O_4 cubane WOCs onto a bismuth vanadate ($BiVO_4$) electrode by drop-casting using Nafion as binder to develop different anodes for photoelectrochemically driven WO. They synthesized a family of Co_4O_4 cubane WOCs by changing the substituent groups on both the pyridine ligands and the alkoxy carboxylato bridging ligands (R_1 and R_2 in WOCs 13 to 21, respectively, Figure 4) to screen different photoanodes for WO. The authors could demonstrate that WO showed a ligand dependent activity that was tuned by modifying the substituent at the Co-WOC immobilized on the WOC/Nafion/$BiVO_4$ photoanode. Among the series, the cubane catalysts featuring long hydrophobic C_4 alkyl chains (to favor direct physisorption) in the alkoxy carboxylato bridging ligands (WOC-20 Figure 4) drop-casted onto $BiVO_4$ was found to be the most active of the series, yielding a photocurrent density for water oxidation of 5 mA cm^{-2} at 1.23 V vs. RHE applied potential under the illumination of simulated sunlight (AM 1.5, 100 mWcm@2) in pH 9.3 borate buffer in a three-electrode configuration, together with a 1.84% solar-to-energy-conversion-a 6-fold enhancement over that of bare $BiVO_4$ [107]. Moreover, the obtained photocurrent was the highest photocurrent for undoped $BiVO_4$ photoanodes and comparable to or even better than those attained by the state-of-the-art metal oxide catalysts. However, the activity started decreasing after 1 h due to slow desorption of the Co-WOC from the electrode during long-term photolysis experiments at 0.7 V vs. RHE applied bias [107].

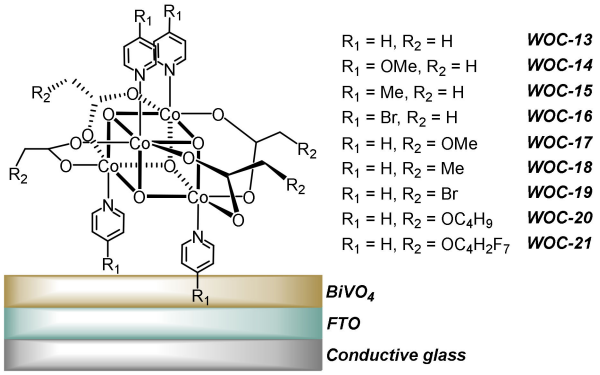

Figure 4. Immobilization of Co water oxidation catalysts onto $BiOVO_4$ derivative photoanodes for photoelectrocatalyzed water oxidation [107].

3.4. Utilization of Physical Confinement Strategies for the Generation of WO (Photo)Anodes

Due to the high porosity, crystallinity, large surface area, modular nature and synthetic versatility MOFs have been widely used for applications in catalysis. Moreover, they have received increasing interest for their use as hosts to stabilize molecular metal complexes for the production of fuels in the field of artificial photosynthesis. For instance, the group of W. Lin pioneered the utilization of MOF-based heterogeneous systems for chemically driven water oxidation upon the incorporation of iridium WOCs into the rigid and protective structure of MOF UiO-67 [146]. Moreover, there are some examples in which MOFs have been used to incorporate molecular WOCs for their application in (photo)electrocatalyzed WO when supported onto electrode surfaces [111,147–150], due to their stabilization effect over the metal complex. For instance, Ott and coworkers reported the incorporation of a $[Ru(tpy)(dcbpy)(OH_2)](ClO_4)_2$ (tpy = 2,2′:6′,2″-terpyridine, dcbpy = 2,2′-bipyridine-5,5′-dicarboxylic acid) catalyst (WOC-22, Figure 5a) into a FTO-grown thin films of the UiO-67 (UiO = University of Oslo) MOF using a post-synthetic ligand exchange approach. The UiO-67-$[Ru(tpy)(dcbpy)(OH_2)](ClO_4)_2$@FTO system evolved O_2 at pH 8.4 at 1.5 V vs. Ag/AgCl applied potential with a FE of 82% and a current density of 11.5 μA cm^{-2} [111]. The system was stable for hours under catalytic conditions, as analyzed by the persistence of the redox wave associated with the $Ru^{III/II}$ couple in the CV indicating the integrity of the catalytic system, which was also supported by powder X-ray diffraction (PXRD) and scanning electron microscopy (SEM) images. Moreover, the catalytic current was stable over multiple scans.

Another system was reported by the group of X-M. Chen, which using post synthetic ion exchange approach to prepare a Co-WOC containing MOF ($[Co_2(\mu\text{-}OH)_2(bbta)]$ (H_2bbta = 1H,5H-benzo-(1,2-d:4,5-d′)bistriazole) that contained both open metal sites as well as hydroxide ligands (WOC-23, Figure 5b) and retained its original crystallinity in either acidic or basic solutions for over a week. This material showed an improved electrocatalytic activity for O_2 evolution obtaining 10.0 mA cm^{-2} at 292 mV overpotential at pH 14 when coated on a glassy carbon electrode using Nafion as binder, which surpassed the activity of its inorganic $Co(OH)_2$ and Co_3O_4 analogues under similar conditions [147]. Isotopic labelling experiments confirmed the role of the hydroxide ligands in the WO reaction, which lowered the energy for the direct coupling pathway.

In the same line, using MOFs as host porous materials, Das and coworkers reported a hybrid metal–organic material $[\{Co_3(\mu_3\text{-}OH)(BTB)_2(dpe)_2\}^{-}\{Co\text{-}(H_2O)_4(DMF)_2\}_{0.5}]_n \cdot nH_2O$ in which the mononuclear positively charged Co-WOC $[Co\text{-}(H_2O)_4(DMF)_2]^{2+}$ (WOC-24, Figure 5c) is encapsulated in the host MOF resulting in a host–guest supramolecular system, where the negative charge of two $\{Co_3(\mu_3\text{-}OH)(COO)_6\}^{-}$ units (inactive for WO) are balanced by the molecular Co WOC-24 (active for WO). This results in the formation of a rigid environment around the active site. This system was coated onto a glassy carbon electrode to explore its catalytic activity towards WO, showing stability in basic media and a remarkable electrocatalytic activity for O_2 evolution with a TOF of 0.05 s^{-1} at 390 mV vs. NHE overpotential at pH 13 with a current density of 1 mA cm^{-2} [148]. Catalytic tests showed the maximum WO activity at pH 13 due to the coordination of hydroxo ligands (OH^{-}) to the mononuclear Co ion, which compensates the extra positive charge of the overall host–guest system. Additionally, mechanistic studies confirmed that only the $[Co\text{-}(H_2O)_4(DMF)_2]^{2+}$ WOC-24 was responsible for the WO activity. Furthermore, stability tests by ICP, EDX and electrochemical studies discarded any leaching of the Co catalyst from the MOF into the electrolyte solution after 1000 catalytic scans, which reaffirms the stability provided by the physical confinement in the guest.

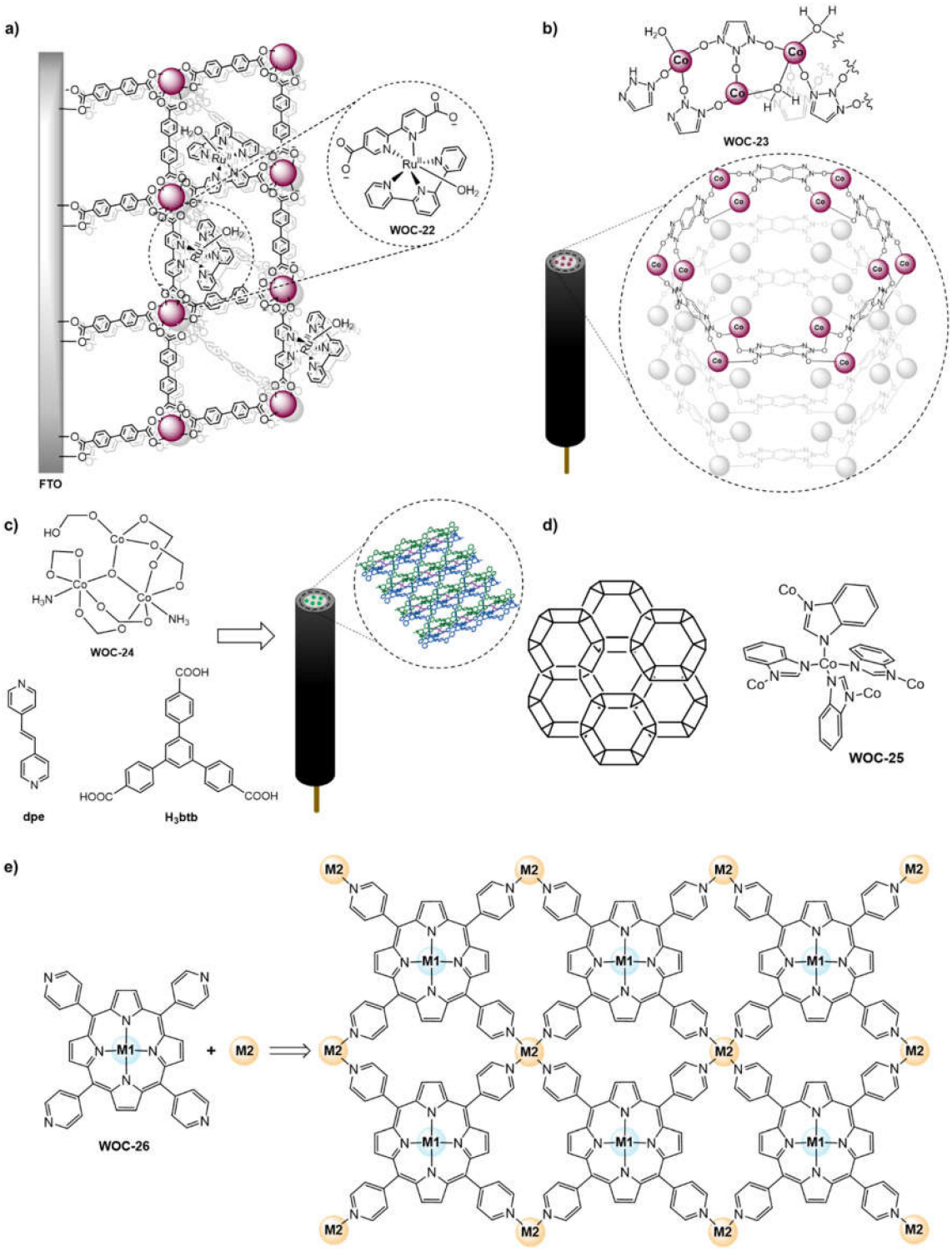

Figure 5. Immobilization of WOCs onto electrodes upon physical confinement in MOFs and COFS. Simplified representation of: (**a**) UiO-67-[Ru(tpy)(dcbpy)(OH_2)](ClO_4)$_2$@FTO [111], (**b**) [Co_2(μ-OH)$_2$(bbta)] MOF containing a Co-WOC [147], (**c**) [{Co_3(μ_3-OH)(BTB)$_2$(dpe)$_2$ {Co-(H_2O)$_4$(DMF)$_2$}$_{0.5}$]$_n$·$n$$H_2O$ MOF [148], (**d**) cobalt zeolitic imidazolate framework [150], and (**e**) the heterobimetallic Fe/Co porphyrin-based MOF (M1 = Fe and M2 = Co for the most active MOF of the series, despite all the possible combinations were screened) [150].

Later on, Wang and coworkers reported a Co-based WOC (WOC-25, Figure 5d) that consisted of a MOF where the redox function of the embedded cobalt active centers was

modified by introducing imidazolate ligands as linkers to facilitate the proton transfer process involved in WO, generating a Co-containing zeolitic imidazolate framework (Co-ZIF) that was supported onto an FTO electrode to explore its electrochemical WO capability. This system showed WO activity at pH 7 with the onset of the catalytic current at 1.6 V vs. RHE (400 mV vs. RHE overpotential), producing 20 TON O2 after 3 h electrolysis with a TOF of $1.76 \cdot 10^{-3}$ s^{-1}. The system remained stable over 25 h operation. Moreover, it was also electrocatalytically active for O_2 evolution in a wide range of pH values. Finally, DFT calculations of the system proved the thermodynamic feasibility of Co-ZIF to activate the water molecule via binding the OH group to the metal sites with low activation barriers, while the eliminated proton was accepted by the nearby benzimidazolate ligands, which was in agreement with the observed reactivity [149].

Kern and coworkers developed novel heterobimetallic MOFs by expanding a porphyrin network using 5,10,15,20-tetra(4-pyridyl)- 21H,23H-porphyrine (TPyP, Figure 5e) and rationally occupying the coordination sites by single iron or cobalt atoms in a specific manner, which was characterized by scanning tunneling microscopy (STM). That is, either with the Fe in the coordination center of the porphyrin while the Co were placed in the corners between four neighboring porphyrins, or by placing the Co atoms in the coordination center and the Fe in the corners (M1-TPyP-M2, WOC-26, Figure 5e) [150]. All the developed MOFs were active for electrochemically driven WO when supported on a gold electrode at pH 13. Moreover, catalytic activity increased dramatically depending on the coordination spheres of Fe and Co, with the heterobimetallic M1-TPyP-M2 MOFs displaying faster reaction kinetics and higher activity for O_2 evolution than the single Fe or Co TPyP porphyrins at 300 mV vs. Ag/AgCl overpotential, which is lower than the prototypical hangman porphyrins for WO (600 mV overpotential). The FeTPyP-Co MOF showed the highest electrocatalytic activity (3.43 nmol O_2 cm^{-2}) and fastest kinetics (12.2 s^{-2} TOF > 15-fold higher than the hangman porphyrin [151]). Mechanistic studies based on electrochemistry and preliminary X-ray absorption spectroscopy (XAS) showed the importance of the coordination environment of the metal centers and the synergistic effect of the two proximate metal centers, as well as suggesting that the pyridyl-Co moiety was a critical site for WO. This highly modular porphyrin-based MOF demonstrated the manifold synthetic possibilities and combinations to explore to develop more highly active heterogenized WOCs by just changing the metal ions and the meso-substituents in the porphyrin.

3.5. Heterogenization of WOCs by Electropolymerization

Among the first examples of electrografted WOCs, Lin et al. reported iridium-based WOC containing a pentamethylcyclopentadienyl (Cp*) ligand and 2,2′-bipyridine or 2-pehnylpyridine ligand with amine pendant groups ([Cp*IrCl(4-NH_2-bpy)]Cl, [Cp*IrCl(5-NH_2-bpy)]Cl and [Cp*IrCl(p-NH_2-ppy)]) that were immobilized onto a glassy carbon electrodes upon diazonium electrografting at −0.4 V vs. NHE applied potential for 4 min on a 1.13 cm^2 planar carbon electrode. The heterogenized systems showed TOFs up to 3.31 s^{-1} when using catalyst [Cp*IrCl(p-NH_2-ppy)] and were proven to be more stable that its homogeneous counterpart and was active without loss of the covalently bound WOC for 3 h and then some catalysts was lost during the electrocatalysis, but this was only apparent after 10 days of electrolysis. This catalyst leaching from the electrode surface was responsible for the depletion of catalytic activity [118].

Then, Meyer and co-workers demonstrated that water-stable photoactive interfaces on TiO_2 electrodes could be prepared by reductive electropolymerization of catalysts onto TiO_2 immobilized dyes. The group reported a Ru dye containing vinyl groups in two of the 2,2′-bipyridine and a carboxylic acid groups in the other $[Ru(vbpy)_2(dcb)](PF_6)_2$ (vbpy = 4-methyl-4′-vinyl-2,2′-bipyridine and dcb = 2,2′-bipyridine-4,4′-dicarboxylic acid) immobilized onto a TiO_2 electrode via the carboxylate groups that was stabilized upon reductive electropolymerization of a $[Ru(vbpy)_2(dppe)](PF_6)_2$ (dppe = cis-1,2-Bis-(diphenylphosphino)ethylene) complex forming an immobilized TiO_2-$[Ru(vbpy)_2(dcb)](PF_6)_2$/poly-$[Ru(vbpy)_2(dppe)](PF_6)_2$

composite. The polymeric layer was transparent to visible light and stable in water that was photoactive and could last for up to 3 weeks [152]. Later on, the same group used this approach to test the stabilization of photosensitizers immobilized onto (photo)electrodes with phosphonate anchoring groups upon electropolymerization of a molecular Fe-based complex onto mesoporous TiO_2 electrodes previously functionalized with [Ru(dvb)$_2$(4,4′-(PO$_3$H$_2$)$_2$-bpy)]Cl$_2$ (dvb = 5,5′-divinyl-2,2′-bipyridine, 4,4′-(PO$_3$H$_2$)$_2$-bpy = [2,2′-bipyridine]-4,4′-diylbis(phosphonic acid)) anchored to TiO_2 through the phosphonate at the 2,2′-bipyridine [153]. A [Fe(v-tpy)$_2$](PF$_6$)$_2$ (v-tpy = 4′-vinyl-2,2′:6′:2″-terpyridine, Fe-1 Figure 6a) complex was reductively electropolymerized onto TiO_2-[Ru(dvb)$_2$(4,4′-(PO$_3$H$_2$)$_2$-bpy)]Cl$_2$ generating an electropolymerized overlayer of TiO_2-[Ru(dvb)$_2$(4,4′-(PO$_3$H$_2$)$_2$-bpy)]Cl$_2$-*poly*-[Fe(v-tpy)$_2$](PF$_6$)$_2$ [153]. This resulted in a 30-fold enhancement of the photostability as compared to the surface-bound dye alone or immobilized via ALD. This example proved the generalization of electropolymerization to stabilize different types of anchored dyes onto electrode surfaces.

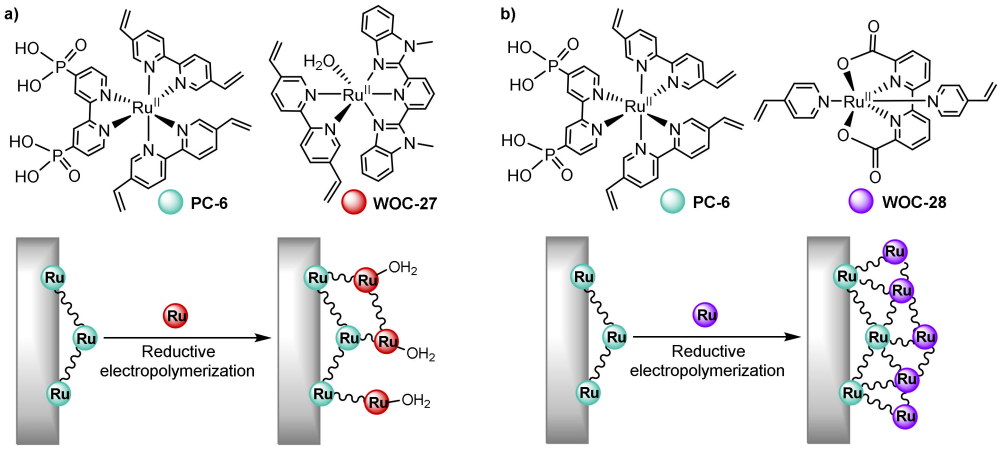

Figure 6. Selected examples of electrodes for WO fabricated via electropolymerization of Ru WOCs onto *n*TiO_2-, *p*FTO- or *n*ITO -[Ru(dvb)$_2$(4,4′-(PO$_3$H$_2$)$_2$-bpy)]Cl$_2$ electrodes: (**a**) [Ru(Mebimpy)-(dvb)(OH$_2$)]$^{2+}$ [116] and (**b**) [Ru(bda)(vpy)$_2$] [154].

Later on, the same group proved the scope of this strategy and demonstrated that Ru-WOCs can be introduced onto those derivatized *n*TiO_2-, *p*FTO- or *n*ITO-[Ru(dvb)$_2$(4,4′-(PO$_3$H$_2$)$_2$-bpy)]Cl$_2$ by reductive electropolymerization of the vinyl groups present in both the photoredox catalyst and the complexes, generating photostable and water stable photoanodes for WO [116,154]. First, they electropolymerized a [Ru(Mebimpy)-(dvb)(OH$_2$)]$^{2+}$ (WOC-27, Mebimpy = 2,6-bis(1-methyl-1H-benzo[d]imidazole-2-yl)pyridine) WOC onto *n*TiO_2-, *p*FTO- or *n*ITO-[Ru(dvb)$_2$(4,4′-(PO$_3$H$_2$)$_2$-bpy)]Cl$_2$ that showed a dramatic increase in photostability up to 16 h (Figure 6a) [116]. The electropolymerization of the Ru-WOC onto the dye-derivatized electrode stabilized and protected the dye from leaching, since the phosphate immobilized dye-oxide surface photoelectrode showed chromophore loss since the beginning of the irradiation time. Electrocatalyzed WO was maintained for more than 2 h using either *n*ITO-*poly*-[Ru(Mebimpy)-(dvb)(OH$_2$)]$^{2+}$ or *n*ITO -[Ru(dvb)$_2$(4,4′-(PO$_3$H$_2$)$_2$-bpy)]Cl$_2$-*poly*-[Ru(Mebimpy)-(dvb)(OH$_2$)]$^{2+}$ with 77% FE and 501 TON O_2 and 0.046 s^{-1} TOF.

After that the same group reported a photocatalytically active photoanode for WO by reductive electropolymerization of a Ru-bda [132] derivative WOC [Ru(bda)(vpy)$_2$] (bda = 2,2′-bipyridine-6,6′-dicarboxylate, vpy = 4-vinylpyridine) on glassy carbon (GC) and*n*TiO_2 electrodes results in films containing semirigid polymer networks that produce sustained water oxidation at pH 7 as measured in real-time by use of a two-electrode cell [119,154]. Using a rotating disk electrode the GC-[Ru(dvb)$_2$(4,4′-(PO$_3$H$_2$)$_2$-bpy)]Cl$_2$-*poly*-[Ru(bda)(vpy)$_2$] produced O_2 with 62% FE at pH 7 with a catalytic onset at 0.95 V vs. SCE, which was consistent with the onset potential of WOC-28 (Figure 6b). With this config-

uration, a TOF of 8.5 s^{-1} was obtained at 1.2 V vs. SCE applied bias (620 mV overpotential). Finally, the system was tested for photocatalyzed WO, using the *n*TiO_2-[Ru(dvb)$_2$(4,4′-(PO_3H_2)$_2$-bpy)]Cl_2-*poly*-[Ru(bda)(vpy)$_2$] photoanode in a DSPEC configuration using a Pt cathode for H_2 production at 0.2 V vs. SCE applied bias, producing O_2 with a FE of 8% under 1 sun illumination (100 mW cm^{-2}) [154]. The study of this system showed that the coordination chemistry and proton-coupled electron-transfer properties (PCET) of complex WOC-28 are maintained upon electropolymerization. However, there is a change in the mechanism for the O–O bond formation from DC in solution to a single-site WNA in the film environment onto the electrodes. This example further reinforced the capacity of this immobilization strategy to heterogenized active WOCs with or without dyes onto electrodes for (photo)electrocatalyzed WO.

3.6. Use of Atomic Layer Deposition for the Fabrication of WO (Photo)Anodes

Templeton, Meyer and coworkers developed the atomic layer deposition (ALD) approach to prepare (photo)anodes in a more efficient manner and rendering more stable hybrids. They prepared a Ru(II) polypyridyl photoredox catalyst and WOC assembly on nanoparticle films of tin-doped indium oxide (*nano*ITO) and titanium dioxide (*nano*TiO_2) for electrocatalytic and photoelectrocatalytic WO, respectively using ALD [119]. First, the photoredox catalyst [Ru(4,4′-(PO_3H_2)$_2$-bpy)(bpy)$_2$]$^{2+}$ (4,4′-(PO_3H_2)$_2$-bpy = [2,2′-bipyridine]-4,4′-diylbis(phosphonic acid) and bpy = 2,2′-bipyridine, PC-1, Figure 7) was coated onto films of *n*ITO and *n*TiO_2 generating *n*ITO | PC-1 and *n*TiO_2 | PC-1, after which overlayers of aluminum oxide (Al_2O_3) were deposited atop the *n*ITO | PC-1 and *n*TiO_2 | PC-1 by ALD to ensure the photostability of the photoredox catalyst. Then, a [Ru(Meipy)(4,4′-($PO_3H_2CH_2$)$_2$-bpy)(OH_2)]$^{2+}$ (Meipy = 2,6-bis(1-methyl-1*H*-benzo[*d*]imidazol-2-yl)pyridine and 4,4′-($PO_3H_2CH_2$)$_2$-bpy = 4,4′-((HO)$_2$(O)P–CH_2)$_2$-2,2′-bipyridine) catalyst (WOC-29, Figure 7) was loaded from a methanol solution onto the *n*ITO | PC-1 | Al_2O_3 and *nano* TiO_2 | -PC-1 | Al_2O_3 and more layers of Al_2O_3 were deposited on top to ensure the electrochemical stability of the Ru WOC. The electrodes were characterized by CV, SEM and UV–vis spectroscopy. Currents higher than 60 μA cm^{-2} and TOF O_2 0.014 s^{-1} (23% FE) were obtained for the *n*ITO | PC-1 | Al_2O_3 | WOC-29 | Al_2O_3 at 1.4 V vs. NHE applied potential, as quantified in a dual working electrode collector-generator cell [119]. However, the current decreased to 20 μA cm^{-2} after 2 h most likely due to ligand decomposition in the Ru WOC at higher oxidation state. Photoelectrochemical studies with *n*TiO_2 | PC-1 | Al_2O_3 | WOC-29 | Al_2O_3 with a white light source at 0.64 V vs. NHE applied potential generated O_2 with at 16.8% FE after 6 h irradiation.

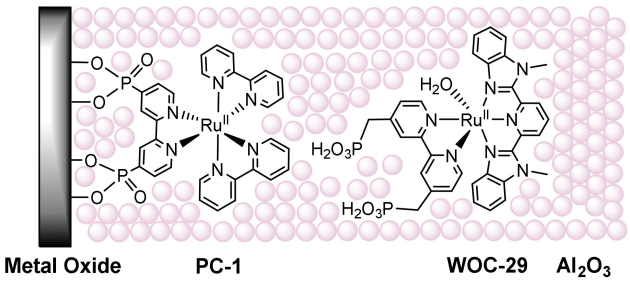

Figure 7. Immobilization of [Ru(Meipy)(4,4′-($PO_3H_2CH_2$)$_2$-bpy)(OH_2)]$^{2+}$ together with [Ru(4,4′-(PO_3H_2)$_2$-bpy)(bpy)$_2$]$^{2+}$ onto *n*ITO and *n*TiO_2 by ALD for electro- and photoelectrocatalyzed WO.

3.7. Use of Layer-by-Layer Deposition to Deposit WOCs onto Electrodes

The groups of Meyer and Schanze and coworkers reported for the first time the assembly of chromophores and WOCs by using the polyelectrolyte layer-by-layer deposition method [55,155]. Their system consists on a cationic polystyrene-based Ru polychromophore (PC-7) and a [Ru(tpy)(pyMebzi)(OH_2)]$^{2+}$ (tpy = 2,2′:6′,2″-terpyridine and pyMebzi = 2-pyridyl-N-methylbenzimidazole) Ru-based catalyst (WOC-30), co-deposited with poly(acrylic acid) (PAA) as an inert polyanion onto planar indium tin oxide (ITO)

substrates for electrochemical characterization and onto mesoporous electrodes consisting of a SnO_2/TiO_2 core/shell structure on top of fluorine doped tin oxide (FTO) for photoelectrochemical water oxidation in a dye-sensitized PEC (Figure 8) [155]. The resulting photoanodes were characterized by CV, UV–vis spectroscopy and SEM. Photoelectrolysis WO experiments were performed using a dual working electrode collector-generator cell [119] to allow for O_2 quantification, obtaining 22% FE for O_2 evolution at 0.44 V vs. NHE applied bias with 1.4 V vs. NHE as the onset for WO.

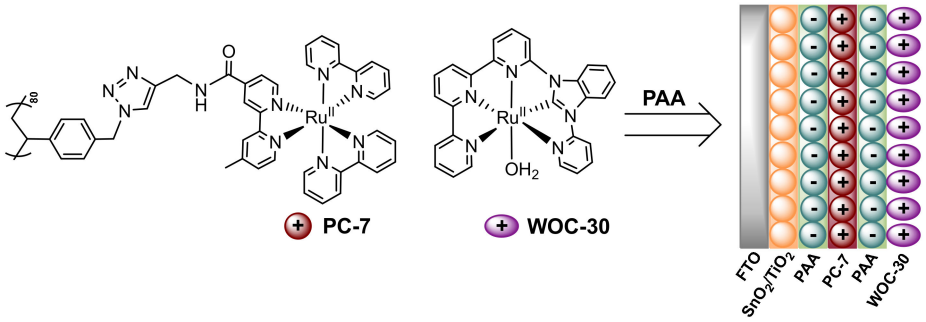

Figure 8. Immobilization of $[Ru(tpy)(pyMebzi)(OH_2)]^{2+}$ together with a cationic polystyrene-based Ru polychromophore onto a FTO-SnO_2/TiO_2 photoelectrode for photoelectrochemical WO by Layer-by-Layer deposition. [155].

4. Conclusions and Perspective

Despite the challenges faced using molecular water oxidation catalysts in artificial photosynthetic devices, the heterogenization of molecular systems onto electrodes for (photo)electrocatalyzed water oxidation has several advantages over their respective homogeneous counterparts but also over heterogeneous systems. For instance, the heterogenization of molecular water oxidation catalysts allows for modular systems based on well-defined molecular WOCs that are easily tunable, while surpassing the long-term stability of their homogeneous counterparts. Moreover, these systems are easier to study and therefore to use to establish common designing principles after analysis of those catalytically active (photo)anodes for WO.

In this review we have seen several methods to immobilize WOCs and WOCs/photoredox catalysts onto different electrode surfaces. Some strategies are preferred over others as the initial properties of the molecular catalysts are preserved and due to the increased stability that they render to the final (photo)anodes. For instance, the use of electrografting or the more recent layer-by-layer deposition offer a more efficient and less synthetically tedious approach to the heterogenization of molecular water oxidation catalysts onto electrodes yielding more stable (photo)anodes. These strategies show those advantages over other approaches such as covalent immobilization which often requires complex synthetic derivatizations and can lead to dramatic changes in the electrochemical and physical properties of the molecular catalysts, which lead to changes in their catalytic performance. Despite the fact that supramolecular approaches can simplify synthetic derivatization procedure, the stability of these assemblies can be more susceptible to the catalytic conditions and hamper applications in artificial photosynthesis where synchronous reduction and oxidation reactions take place. It is worth mentioning that the revised immobilization strategies can also be applied to other catalysts beyond WO and there are several examples reported elsewhere.

To develop photoanodes for WO via heterogenization of molecular WOCs for practical applications, special attention needs to be put in the preservation of catalytic activity after immobilization onto electrode surfaces, as well as the stability of the assembly in the long term under (photo)catalytic conditions. Moreover, an overall improvement of the photo-driven catalytic activity is desired upon coimmobilization of dyes and WOCs onto electrodes for efficient and sustained WO. Despite some advances in the field of immobi-

lization of molecular WOCs for artificial photosynthetic devices, future progress is needed in the development of (photo)anodes based on non-precious metal-based WOCs with high efficiency and catalytic activity at low overpotentials, long-term stability and durability.

Funding: This research received no external funding.

Institutional Review Board Statement: Not applicable.

Informed Consent Statement: Not applicable.

Data Availability Statement: Not applicable.

Acknowledgments: The European Commission is acknowledged for a Marie Skłodowska-Curie Individual Fellowship (890745-SmArtC).

Conflicts of Interest: The author declares no conflict of interest.

References

1. Masson-Delmotte, V.; Zhai, P.; Pörtner, H.-O.; Roberts, D.; Skea, J.; Shukla, P.R.; Pirani, A.; Moufouma-Okia, W.; Péan, C.; Pidcock, R.S.; et al. *Global Warming of 1.5 °C. An IPCC Special Report on the Impacts of Global Warming of 1.5 °C above Pre-Industrial Levels and Related Global Greenhouse Gas Emission Pathways, in the Context of Strengthening the Global Response to the Threat of Climate Change, Sustainable Development, and Efforts to Eradicate Poverty*; IPCC special report on the impacts of global warming; IPCC: Geneva, Switzerland, 2018.
2. Field, C.B.; Behrenfeld, M.J.; Randerson, J.T.; Falkowski, P. Primary Production of the Biosphere: Integrating Terrestrial and Oceanic Components. *Science* **1998**, *281*, 237–240. [CrossRef] [PubMed]
3. Lewis, N.S. Research opportunities to advance solar energy utilization. *Science* **2016**, *351*, aad1920. [CrossRef]
4. Schultz, D.M.; Yoon, T.P. Solar Synthesis: Prospects in Visible Light Photocatalysis. *Science* **2014**, *343*, 1239176. [CrossRef] [PubMed]
5. Zhang, B.; Sun, L. Artificial photosynthesis: Opportunities and challenges of molecular catalysts. *Chem. Soc. Rev.* **2019**, *48*, 2216–2264. [CrossRef] [PubMed]
6. Cox, N.; Pantazis, D.A.; Lubitz, W. Current Understanding of the Mechanism of Water Oxidation in Photosystem II and Its Relation to XFEL Data. *Annu. Rev. Biochem.* **2020**, *89*, 795–820. [CrossRef] [PubMed]
7. Crowe, S.A.; Døssing, L.N.; Beukes, N.J.; Bau, M.; Kruger, S.J.; Frei, R.; Canfield, D.E. Atmospheric oxygenation three billion years ago. *Nature* **2013**, *501*, 535–538. [CrossRef] [PubMed]
8. Amunts, A.; Drory, O.; Nelson, N. The structure of a plant photosystem I supercomplex at 3.4 Å resolution. *Nature* **2007**, *447*, 58–63. [CrossRef]
9. Umena, Y.; Kawakami, K.; Shen, J.R.; Kamiya, N. Crystal structure of oxygen–evolving photosystem II at a resolution of 1.9 Å. *Nature* **2011**, *473*, 55–60. [CrossRef]
10. Kornienko, N.; Zhang, J.Z.; Sakimoto, K.K.; Yang, P.; Reisner, E. Interfacing nature's catalytic machinery with synthetic materials for semi–artificial photosynthesis. *Nat. Nanotechnol.* **2018**, *13*, 890–899. [CrossRef]
11. Zhang, J.Z.; Sokol, K.P.; Paul, N.; Romero, E.; van Grondelle, R.; Reisner, E. Competing charge transfer pathways at the photosystem II–electrode interface. *Nat. Chem. Biol.* **2016**, *12*, 1046. [CrossRef]
12. Schwizer, F.; Okamoto, Y.; Heinisch, T.; Gu, Y.; Pellizzoni, M.M.; Lebrun, V.; Reuter, R.; Köhler, V.; Lewis, J.C.; Ward, T.R. Artificial Metalloenzymes: Reaction Scope and Optimization Strategies. *Chem. Rev.* **2018**, *118*, 142–231. [CrossRef]
13. Bonke, S.A.; Wiechen, M.; MacFarlane, D.R.; Spiccia, L. Renewable fuels from concentrated solar power: Towards practical artificial photosynthesis. *Energy Environ. Sci.* **2015**, *8*, 2791–2796. [CrossRef]
14. Michel, H. Editorial: The Nonsense of Biofuels. *Angew. Chem. Int. Ed.* **2012**, *51*, 2516–2518. [CrossRef] [PubMed]
15. Qiu, B.; Du, M.; Ma, Y.; Zhu, Q.; Xing, M.; Zhang, J. Integration of redox cocatalysts for artificial photosynthesis. *Energy Environ. Sci.* **2021**, *14*, 5260–5288. [CrossRef]
16. Li, F.; Yang, H.; Li, W.; Sun, L. Device Fabrication for Water Oxidation, Hydrogen Generation, and CO_2 Reduction via Molecular Engineering. *Joule* **2018**, *2*, 36–60. [CrossRef]
17. Villa, K.; Galán–Mascarós, J.R.; López, N.; Palomares, E. Photocatalytic water splitting: Advantages and challenges. *Sustain. Energy Fuels* **2021**, *5*, 4560–4569. [CrossRef]
18. Li, Y.; Du, X.; Huang, J.; Wu, C.; Sun, Y.; Zou, G.; Yang, C.; Xiong, J. Recent Progress on Surface Reconstruction of Earth–Abundant Electrocatalysts for Water Oxidation. *Small* **2019**, *15*, 1901980. [CrossRef]
19. Casadevall, C.; Bucci, A.; Costas, M.; Lloret–Fillol, J. Chapter Four—Water oxidation catalysis with well–defined molecular iron complexes. In *Advances in Inorganic Chemistry*; Eldik, R., Hubbard, C.D., Eds.; Academic Press: Cambridge, MA, USA, 2019; Volume 74, pp. 151–196.
20. Kato, N.; Mizuno, S.; Shiozawa, M.; Nojiri, N.; Kawai, Y.; Fukumoto, K.; Morikawa, T.; Takeda, Y. A large–sized cell for solar–driven CO_2 conversion with a solar-to-formate conversion efficiency of 7.2%. *Joule* **2021**, *5*, 687–705. [CrossRef]

21. Qiao, J.; Liu, Y.; Hong, F.; Zhang, J. A review of catalysts for the electroreduction of carbon dioxide to produce low–carbon fuels. *Chem. Soc. Rev.* **2014**, *43*, 631–675. [CrossRef]
22. Franco, F.; Rettenmaier, C.; Jeon, H.S.; Roldan Cuenya, B. Transition metal–based catalysts for the electrochemical CO_2 reduction: From atoms and molecules to nanostructured materials. *Chem. Soc. Rev.* **2020**, *49*, 6884–6946. [CrossRef]
23. Franco, F.; Fernández, S.; Lloret–Fillol, J. Advances in the electrochemical catalytic reduction of CO_2 with metal complexes. *Curr. Opin. Electrochem.* **2019**, *15*, 109–117. [CrossRef]
24. Kim, J.H.; Hansora, D.; Sharma, P.; Jang, J.–W.; Lee, J.S. Toward practical solar hydrogen production—an artificial photosynthetic leaf–to–farm challenge. *Chem. Soc. Rev.* **2019**, *48*, 1908–1971. [CrossRef] [PubMed]
25. Jessop, P.G.; Ikariya, T.; Noyori, R. Homogeneous Hydrogenation of Carbon Dioxide. *Chem. Rev.* **1995**, *95*, 259–272. [CrossRef]
26. Liu, Q.; Wu, L.; Jackstell, R.; Beller, M. Using carbon dioxide as a building block in organic synthesis. *Nat. Commun.* **2015**, *6*, 5933. [CrossRef]
27. Centi, G.; Perathoner, S. Opportunities and prospects in the chemical recycling of carbon dioxide to fuels. *Catal. Today* **2009**, *148*, 191–205. [CrossRef]
28. Garrido-Barros, P.; Matheu, R.; Gimbert-Suriñach, C.; Llobet, A. Electronic, mechanistic, and structural factors that influence the performance of molecular water oxidation catalysts anchored on electrode surfaces. *Curr. Opin. Electrochem.* **2019**, *15*, 140–147. [CrossRef]
29. Godwin, I.; Rovetta, A.; Lyons, M.; Coleman, J. Electrochemical water oxidation: The next five years. *Curr. Opin. Electrochem.* **2018**, *7*, 31–35. [CrossRef]
30. Bairagya, M.D.; Bujol, R.J.; Elgrishi, N. Fighting Deactivation: Classical and Emerging Strategies for Efficient Stabilization of Molecular Electrocatalysts. *Chem. A Eur. J.* **2020**, *26*, 3991–4000. [CrossRef]
31. Bullock, R.M.; Das, A.K.; Appel, A.M. Surface Immobilization of Molecular Electrocatalysts for Energy Conversion. *Chem. A Eur. J.* **2017**, *23*, 7626–7641. [CrossRef]
32. Lubitz, W.; Chrysina, M.; Cox, N. Water oxidation in photosystem II. *Photosynth. Res.* **2019**, *142*, 105–125. [CrossRef]
33. Cox, N.; Pantazis, D.A.; Neese, F.; Lubitz, W. Biological Water Oxidation. *Acc. Chem. Res.* **2013**, *46*, 1588–1596. [CrossRef]
34. Blakemore, J.D.; Crabtree, R.H.; Brudvig, G.W. Molecular Catalysts for Water Oxidation. *Chem. Rev.* **2015**, *115*, 12974–13005. [CrossRef] [PubMed]
35. Kärkäs, M.D.; Verho, O.; Johnston, E.V.; Åkermark, B. Artificial Photosynthesis: Molecular Systems for Catalytic Water Oxidation. *Chem. Rev.* **2014**, *114*, 11863–12001. [CrossRef] [PubMed]
36. Fukuzumi, S.; Kojima, T.; Lee, Y.-M.; Nam, W. High-valent metal-oxo complexes generated in catalytic oxidation reactions using water as an oxygen source. *Coord. Chem. Rev.* **2017**, *333*, 44–56. [CrossRef]
37. Casadevall, C.; Codolà, Z.; Costas, M.; Lloret-Fillol, J. Spectroscopic, Electrochemical and Computational Characterisation of Ru Species Involved in Catalytic Water Oxidation: Evidence for a [RuV(O)(Py2Metacn)] Intermediate. *Chem. A Eur. J.* **2016**, *22*, 10111–10126. [CrossRef]
38. Lloret–Fillol, J.; Costas, M. Chapter One—Water oxidation at base metal molecular catalysts. In *Advances in Organometallic Chemistry*; Pérez, P.J., Ed.; Academic Press: Cambridge, MA, USA, 2019; Volume 71, pp. 1–52.
39. Meyer, T.J.; Sheridan, M.V.; Sherman, B.D. Mechanisms of molecular water oxidation in solution and on oxide surfaces. *Chem. Soc. Rev.* **2017**, *46*, 6148–6169. [CrossRef]
40. Casadevall, C.; Martin-Diaconescu, V.; Browne, W.R.; Fernández, S.; Franco, F.; Cabello, N.; Benet-Buchholz, J.; Lassalle-Kaiser, B.; Lloret-Fillol, J. Isolation of a Ru(iv) side–on peroxo intermediate in the water oxidation reaction. *Nat. Chem.* **2021**, *13*, 800–804. [CrossRef]
41. Codolà, Z.; Gamba, I.; Acuña-Parés, F.; Casadevall, C.; Clémancey, M.; Latour, J.-M.; Luis, J.M.; Lloret-Fillol, J.; Costas, M. Design of Iron Coordination Complexes as Highly Active Homogenous Water Oxidation Catalysts by Deuteration of Oxidation-Sensitive Sites. *J. Am. Chem. Soc.* **2019**, *141*, 323–333. [CrossRef]
42. Rüdiger, O.; Levin, N.; Casadevall, C.; Cutsail, G.E.; Lloret-Fillol, J.; DeBeer, S. XAS and EPR in situ observation of Ru(V) oxo intermediate in a Ru water oxidation complex. *ChemElectroChem* **2021**, e202101271. [CrossRef]
43. Hessels, J.; Detz, R.J.; Koper, M.T.M.; Reek, J.N.H. Rational Design Rules for Molecular Water Oxidation Catalysts based on Scaling Relationships. *Chem. A Eur. J.* **2017**, *23*, 16413–16418. [CrossRef]
44. Duan, L.; Bozoglian, F.; Mandal, S.; Stewart, B.; Privalov, T.; Llobet, A.; Sun, L. A molecular ruthenium catalyst with water–oxidation activity comparable to that of photosystem II. *Nat. Chem.* **2012**, *4*, 418–423. [CrossRef] [PubMed]
45. Duan, L.; Wang, L.; Li, F.; Li, F.; Sun, L. Highly Efficient Bioinspired Molecular Ru Water Oxidation Catalysts with Negatively Charged Backbone Ligands. *Acc. Chem. Res.* **2015**, *48*, 2084–2096. [CrossRef] [PubMed]
46. Wang, L.; Duan, L.; Ambre, R.B.; Daniel, Q.; Chen, H.; Sun, J.; Das, B.; Thapper, A.; Uhlig, J.; Dinér, P.; et al. A nickel (II) PY5 complex as an electrocatalyst for water oxidation. *J. Catal.* **2016**, *335*, 72–78. [CrossRef]
47. Geletii, Y.V.; Botar, B.; Kögerler, P.; Hillesheim, D.A.; Musaev, D.G.; Hill, C.L. An All-Inorganic, Stable, and Highly Active Tetraruthenium Homogeneous Catalyst for Water Oxidation. *Angew. Chem. Int. Ed.* **2008**, *47*, 3896–3899. [CrossRef] [PubMed]
48. Azmani, K.; Besora, M.; Soriano-López, J.; Landolsi, M.; Teillout, A.-L.; de Oliveira, P.; Mbomekallé, I.-M.; Poblet, J.M.; Galán-Mascarós, J.-R. Understanding polyoxometalates as water oxidation catalysts through iron vs. cobalt reactivity. *Chem. Sci.* **2021**, *12*, 8755–8766. [CrossRef] [PubMed]

49. Lv, H.; Geletii, Y.V.; Zhao, C.; Vickers, J.W.; Zhu, G.; Luo, Z.; Song, J.; Lian, T.; Musaev, D.G.; Hill, C.L. Polyoxometalate water oxidation catalysts and the production of green fuel. *Chem. Soc. Rev.* **2012**, *41*, 7572–7589. [CrossRef]
50. Li, P.; Zhao, R.; Chen, H.; Wang, H.; Wei, P.; Huang, H.; Liu, Q.; Li, T.; Shi, X.; Zhang, Y.; et al. Recent Advances in the Development of Water Oxidation Electrocatalysts at Mild pH. *Small* **2019**, *15*, 1805103. [CrossRef]
51. Bo, X.; Dastafkan, K.; Zhao, C. Design of Multi-Metallic-Based Electrocatalysts for Enhanced Water Oxidation. *Chemphyschem* **2019**, *20*, 2936–2945. [CrossRef]
52. Lei, Z.; Wang, T.; Zhao, B.; Cai, W.; Liu, Y.; Jiao, S.; Li, Q.; Cao, R.; Liu, M. Recent Progress in Electrocatalysts for Acidic Water Oxidation. *Adv. Energy Mater.* **2020**, *10*, 2000478. [CrossRef]
53. Song, N.; Concepcion, J.J.; Binstead, R.A.; Rudd, J.; Vannucci, A.K.; Dares, C.J.; Coggins, M.K.; Meyer, T.J. Base-enhanced catalytic water oxidation by a carboxylate-bipyridine Ru(II) complex. *Proc. Natl. Acad. Sci. USA* **2015**, *112*, 4935–4940. [CrossRef]
54. Matheu, R.; Garrido-Barros, P.; Gil-Sepulcre, M.; Ertem, M.Z.; Sala, X.; Gimbert-Suriñach, C.; Llobet, A. The development of molecular water oxidation catalysts. *Nat. Rev. Chem.* **2019**, *3*, 331–341. [CrossRef]
55. Bae, S.; Jang, J.-E.; Lee, H.-W.; Ryu, J. Tailored Assembly of Molecular Water Oxidation Catalysts on Photoelectrodes for Artificial Photosynthesis. *Eur. J. Inorg. Chem.* **2019**, *2019*, 2040–2057. [CrossRef]
56. Zhang, H.; Tian, W.; Duan, X.; Sun, H.; Liu, S.; Wang, S. Catalysis of a Single Transition Metal Site for Water Oxidation: From Mononuclear Molecules to Single Atoms. *Adv. Mater.* **2020**, *32*, 1904037. [CrossRef]
57. Lyons, M.E.G.; Doyle, R.L.; Browne, M.P.; Godwin, I.J.; Rovetta, A.A.S. Recent developments in electrochemical water oxidation. *Curr. Opin. Electrochem.* **2017**, *1*, 40–45. [CrossRef]
58. Lee, K.J.; McCarthy, B.D.; Dempsey, J.L. On decomposition, degradation, and voltammetric deviation: The electrochemist's field guide to identifying precatalyst transformation. *Chem. Soc. Rev.* **2019**, *48*, 2927–2945. [CrossRef] [PubMed]
59. Lee, K.J.; Elgrishi, N.; Kandemir, B.; Dempsey, J.L. Electrochemical and spectroscopic methods for evaluating molecular electrocatalysts. *Nat. Rev. Chem.* **2017**, *1*, 0039. [CrossRef]
60. Zahran, Z.N.; Tsubonouchi, Y.; Mohamed, E.A.; Yagi, M. Recent Advances in the Development of Molecular Catalyst-Based Anodes for Water Oxidation toward Artificial Photosynthesis. *ChemSusChem* **2019**, *12*, 1775–1793. [CrossRef] [PubMed]
61. Lee, H.; Wu, X.; Sun, L. Copper-based homogeneous and heterogeneous catalysts for electrochemical water oxidation. *Nanoscale* **2020**, *12*, 4187–4218. [CrossRef] [PubMed]
62. Materna, K.L.; Crabtree, R.H.; Brudvig, G.W. Anchoring groups for photocatalytic water oxidation on metal oxide surfaces. *Chem. Soc. Rev.* **2017**, *46*, 6099–6110. [CrossRef]
63. Zhang, L.; Cole, J.M. Anchoring Groups for Dye-Sensitized Solar Cells. *ACS Appl. Mater. Interfaces* **2015**, *7*, 3427–3455. [CrossRef]
64. Luitel, T.; Zamborini, F.P. Covalent Modification of Photoanodes for Stable Dye–Sensitized Solar Cells. *Langmuir* **2013**, *29*, 13582–13594. [CrossRef] [PubMed]
65. Savini, A.; Bucci, A.; Nocchetti, M.; Vivani, R.; Idriss, H.; Macchioni, A. Activity and Recyclability of an Iridium-EDTA Water Oxidation Catalyst Immobilized onto Rutile TiO_2. *ACS Catal.* **2015**, *5*, 264–271. [CrossRef]
66. Hara, K.; Sugihara, H.; Tachibana, Y.; Islam, A.; Yanagida, M.; Sayama, K.; Arakawa, H.; Fujihashi, G.; Horiguchi, A.T.; Kinoshita, T. Dye-Sensitized Nanocrystalline TiO_2 Solar Cells Based on Ruthenium(II) Phenanthroline Complex Photosensitizers. *Langmuir* **2001**, *17*, 5992–5999. [CrossRef]
67. Hanson, K.; Brennaman, M.K.; Luo, H.; Glasson, C.R.K.; Concepcion, J.J.; Song, W.; Meyer, T.J. Photostability of Phosphonate–Derivatized, RuII Polypyridyl Complexes on Metal Oxide Surfaces. *ACS Appl. Mater. Interfaces* **2012**, *4*, 1462–1469. [CrossRef] [PubMed]
68. Hanson, K.; Brennaman, M.K.; Ito, A.; Luo, H.; Song, W.; Parker, K.A.; Ghosh, R.; Norris, M.R.; Glasson, C.R.K.; Concepcion, J.J.; et al. Structure–Property Relationships in Phosphonate-Derivatized, RuII Polypyridyl Dyes on Metal Oxide Surfaces in an Aqueous Environment. *J. Phys. Chem. C* **2012**, *116*, 14837–14847. [CrossRef]
69. Zhong, D.K.; Zhao, S.; Polyansky, D.E.; Fujita, E. Diminished photoisomerization of active ruthenium water oxidation catalyst by anchoring to metal oxide electrodes. *J. Catal.* **2013**, *307*, 140–147. [CrossRef]
70. Zhang, L.; Cole, J.M.; Dai, C. Variation in Optoelectronic Properties of Azo Dye-Sensitized TiO_2 Semiconductor Interfaces with Different Adsorption Anchors: Carboxylate, Sulfonate, Hydroxyl and Pyridyl Groups. *ACS Appl. Mater. Interfaces* **2014**, *6*, 7535–7546. [CrossRef]
71. Chen, Y.-S.; Li, C.; Zeng, Z.-H.; Wang, W.-B.; Wang, X.-S.; Zhang, B.-W. Efficient electron injection due to a special adsorbing group's combination of carboxyl and hydroxyl: Dye-sensitized solar cells based on new hemicyanine dyes. *J. Mater. Chem.* **2005**, *15*, 1654–1661. [CrossRef]
72. Wang, D.; Sampaio, R.N.; Troian-Gautier, L.; Marquard, S.L.; Farnum, B.H.; Sherman, B.D.; Sheridan, M.V.; Dares, C.J.; Meyer, G.J.; Meyer, T.J. Molecular Photoelectrode for Water Oxidation Inspired by Photosystem II. *J. Am. Chem. Soc.* **2019**, *141*, 7926–7933. [CrossRef]
73. Antón-García, D.; Warnan, J.; Reisner, E. A diketopyrrolopyrrole dye-based dyad on a porous TiO2 photoanode for solar-driven water oxidation. *Chem. Sci.* **2020**, *11*, 12769–12776. [CrossRef]
74. Wang, D.; Farnum, B.H.; Dares, C.J.; Meyer, T.J. Chemical approaches to artificial photosynthesis: A molecular, dye–sensitized photoanode for O2 production prepared by layer-by-layer self-assembly. *J. Chem. Phys.* **2020**, *152*, 244706. [CrossRef] [PubMed]

75. Wang, D.; Marquard, S.L.; Troian-Gautier, L.; Sheridan, M.V.; Sherman, B.D.; Wang, Y.; Eberhart, M.S.; Farnum, B.H.; Dares, C.J.; Meyer, T.J. Interfacial Deposition of Ru(II) Bipyridine-Dicarboxylate Complexes by Ligand Substitution for Applications in Water Oxidation Catalysis. *J. Am. Chem. Soc.* **2018**, *140*, 719–726. [CrossRef] [PubMed]
76. Fan, K.; Li, F.; Wang, L.; Daniel, Q.; Gabrielsson, E.; Sun, L. Pt-free tandem molecular photoelectrochemical cells for water splitting driven by visible light. *Phys. Chem. Chem. Phys.* **2014**, *16*, 25234–25240. [CrossRef] [PubMed]
77. Brown, D.G.; Schauer, P.A.; Borau-Garcia, J.; Fancy, B.R.; Berlinguette, C.P. Stabilization of ruthenium sensitizers to TiO2 surfaces through cooperative anchoring groups. *J. Am. Chem Soc.* **2013**, *135*, 1692–1695. [CrossRef] [PubMed]
78. Fan, K.; Li, F.; Wang, L.; Daniel, Q.; Chen, H.; Gabrielsson, E.; Sun, J.; Sun, L. Immobilization of a Molecular Ruthenium Catalyst on Hematite Nanorod Arrays for Water Oxidation with Stable Photocurrent. *ChemSusChem* **2015**, *8*, 3242–3247. [CrossRef]
79. Klepser, B.M.; Bartlett, B.M. Anchoring a Molecular Iron Catalyst to Solar-Responsive WO3 Improves the Rate and Selectivity of Photoelectrochemical Water Oxidation. *J. Am. Chem. Soc.* **2014**, *136*, 1694–1697. [CrossRef]
80. Ohshita, J.; Adachi, Y.; Tanaka, D.; Nakashima, M.; Ooyama, Y. Synthesis of D-A polymers with a disilanobithiophene donor and a pyridine or pyrazine acceptor and their applications to dye-sensitized solar cells. *RSC Adv.* **2015**, *5*, 36673–36679. [CrossRef]
81. Casarin, L.; Swords, W.B.; Caramori, S.; Bignozzi, C.A.; Meyer, G.J. Rapid Static Sensitizer Regeneration Enabled by Ion Pairing. *Inorg. Chem.* **2017**, *56*, 7324–7327. [CrossRef]
82. Das, B.; Thapper, A.; Ott, S.; Colbran, S.B. Structural features of molecular electrocatalysts in multi-electron redox processes for renewable energy-recent advances. *Sustain. Energy Fuels* **2019**, *3*, 2159–2175. [CrossRef]
83. Cho, I.; Koshika, M.; Wagner, P.; Koumura, N.; Innis, P.C.; Mori, S.; Mozer, A.J. Exploiting Intermolecular Interactions between Alkyl-Functionalized Redox-Active Molecule Pairs to Enhance Interfacial Electron Transfer. *J. Am. Chem. Soc.* **2018**, *140*, 13935–13944. [CrossRef]
84. Chai, Q.; Li, W.; Wu, Y.; Pei, K.; Liu, J.; Geng, Z.; Tian, H.; Zhu, W. Effect of a Long Alkyl Group on Cyclopentadithiophene as a Conjugated Bridge for D-A-π-A Organic Sensitizers: IPCE, Electron Diffusion Length, and Charge Recombination. *ACS Appl. Mater. Interfaces* **2014**, *6*, 14621–14630. [CrossRef]
85. Brennan, B.J.; Keirstead, A.E.; Liddell, P.A.; Vail, S.A.; Moore, T.A.; Moore, A.L.; Gust, D. 1-(3'-Amino)propylsilatrane derivatives as covalent surface linkers to nanoparticulate metal oxide films for use in photoelectrochemical cells. *Nanotechnology* **2009**, *20*, 505203. [CrossRef] [PubMed]
86. Cecconi, B.; Mordini, A.; Reginato, G.; Zani, L.; Taddei, M.; de Biani, F.F.; De Angelis, F.; Marotta, G.; Salvatori, P.; Calamante, M. Pyridine-N-Oxide 2-Carboxylic Acid: An Acceptor Group for Organic Sensitizers with Enhanced Anchoring Stability in Dye–Sensitized Solar Cells. *Asian J. Org. Chem.* **2014**, *3*, 140–152. [CrossRef]
87. Behar, D.; Frei, H.; Macnaughtan, M.; Rabani, J. Determination of the Redox Potential of Immobilized Oxo–Bridged Metals in Porous Supports. The Ti-O-Mn-SBA System. *J. Phys. Chem. C* **2012**, *116*, 23477–23484. [CrossRef]
88. Materna, K.L.; Jiang, J.; Crabtree, R.H.; Brudvig, G.W. Silatrane Anchors for Metal Oxide Surfaces: Optimization for Potential Photocatalytic and Electrocatalytic Applications. *ACS Appl. Mater. Interfaces* **2019**, *11*, 5602–5609. [CrossRef] [PubMed]
89. Troiano, J.L.; Hu, G.; Crabtree, R.H.; Brudvig, G.W. Diazo coupling for surface attachment of small molecules to TiO_2 nanoparticles. *Chem. Commun.* **2020**, *56*, 9340–9343. [CrossRef]
90. Pandit, B.; Luitel, T.; Cummins, D.R.; Thapa, A.K.; Druffel, T.; Zamborini, F.; Liu, J. Spectroscopic Investigation of Photoinduced Charge-Transfer Processes in FTO/TiO_2/N719 Photoanodes with and without Covalent Attachment through Silane-Based Linkers. *J. Phys. Chem. A* **2013**, *117*, 13513–13523. [CrossRef]
91. Gao, Y.; Ding, X.; Liu, J.; Wang, L.; Lu, Z.; Li, L.; Sun, L. Visible Light Driven Water Splitting in a Molecular Device with Unprecedentedly High Photocurrent Density. *J. Am. Chem. Soc.* **2013**, *135*, 4219–4222. [CrossRef]
92. Lauinger, S.M.; Sumliner, J.M.; Yin, Q.; Xu, Z.; Liang, G.; Glass, E.N.; Lian, T.; Hill, C.L. High Stability of Immobilized Polyoxometalates on TiO2 Nanoparticles and Nanoporous Films for Robust, Light-Induced Water Oxidation. *Chem. Mater.* **2015**, *27*, 5886–5891. [CrossRef]
93. Weng, B.; Yang, M.-Q.; Zhang, N.; Xu, Y.-J. Toward the enhanced photoactivity and photostability of ZnO nanospheres via intimate surface coating with reduced graphene oxide. *J. Mater. Chem. A* **2014**, *2*, 9380–9389. [CrossRef]
94. Wang, F.; Zhou, Y.; Pan, X.; Lu, B.; Huang, J.; Ye, Z. Enhanced photocatalytic properties of ZnO nanorods by electrostatic self–assembly with reduced graphene oxide. *Phys. Chem. Chem. Phys.* **2018**, *20*, 6959–6969. [CrossRef] [PubMed]
95. Singh, Z.; Donnarumma, P.R.; Majewski, M.B. Molecular Copper(I)-Copper(II) Photosensitizer-Catalyst Photoelectrode for Water Oxidation. *Inorg. Chem.* **2020**, *59*, 12994–12999. [CrossRef] [PubMed]
96. Wu, L.; Eberhart, M.; Nayak, A.; Brennaman, M.K.; Shan, B.; Meyer, T.J. A Molecular Silane-Derivatized Ru(II) Catalyst for Photoelectrochemical Water Oxidation. *J. Am. Chem. Soc.* **2018**, *140*, 15062–15069. [CrossRef] [PubMed]
97. Keijer, T.; Bouwens, T.; Hessels, J.; Reek, J.N.H. Supramolecular strategies in artificial photosynthesis. *Chem. Sci.* **2021**, *12*, 50–70. [CrossRef] [PubMed]
98. Yu, F.; Poole, D.; Mathew, S.; Yan, N.; Hessels, J.; Orth, N.; Ivanović-Burmazović, I.; Reek, J.N.H. Control over Electrochemical Water Oxidation Catalysis by Preorganization of Molecular Ruthenium Catalysts in Self-Assembled Nanospheres. *Angew. Chem. Int. Ed.* **2018**, *57*, 11247–11251. [CrossRef]
99. Richmond, C.J.; Matheu, R.; Poater, A.; Falivene, L.; Benet-Buchholz, J.; Sala, X.; Cavallo, L.; Llobet, A. Supramolecular Water Oxidation with Ru-bda-Based Catalysts. *Chem. A Eur. J.* **2014**, *20*, 17282–17286. [CrossRef]

100. Yang, B.; Jiang, X.; Guo, Q.; Lei, T.; Zhang, L.; Chen, B.; Tung, C.; Wu, L. Self-Assembled Amphiphilic Water Oxidation Catalysts: Control of O-O Bond Formation Pathways by Different Aggregation Patterns. *Angew. Chem. Int. Ed.* **2016**, *55*, 6229–6234. [CrossRef]
101. Li, B.; Li, F.; Bai, S.; Wang, Z.; Sun, L.; Yang, Q.; Li, C. Oxygen evolution from water oxidation on molecular catalysts confined in the nanocages of mesoporous silicas. *Energy Environ. Sci.* **2012**, *5*, 8229–8233. [CrossRef]
102. Kunz, V.; Lindner, J.O.; Schulze, M.; Röhr, M.I.S.; Schmidt, D.; Mitrić, R.; Würthner, F. Cooperative water oxidation catalysis in a series of trinuclear metallosupramolecular ruthenium macrocycles. *Energy Environ. Sci.* **2017**, *10*, 2137–2153. [CrossRef]
103. Wang, L.; Polyansky, D.E.; Concepcion, J.J. Self-Assembled Bilayers as an Anchoring Strategy: Catalysts, Chromophores, and Chromophore-Catalyst Assemblies. *J. Am. Chem. Soc.* **2019**, *141*, 8020–8024. [CrossRef]
104. Fukuzumi, S.; Lee, Y.-M.; Nam, W. Immobilization of Molecular Catalysts for Enhanced Redox Catalysis. *ChemCatChem* **2018**, *10*, 1686–1702. [CrossRef]
105. Mantovani, K.M.; Molgero Westrup, K.C.; da Silva Junior, R.M.; Jaerger, S.; Wypych, F.; Nakagaki, S. Oxidation catalyst obtained by the immobilization of layered double hydroxide/Mn(iii) porphyrin on monodispersed silica spheres. *Dalton Trans.* **2018**, *47*, 3068–3073. [CrossRef] [PubMed]
106. Kaliyaraj Selva Kumar, A.; Zhang, Y.; Li, D.; Compton, R.G. A mini-review: How reliable is the drop casting technique? *Electrochem. Commun.* **2020**, *121*, 106867. [CrossRef]
107. Wang, Y.; Li, F.; Zhou, X.; Yu, F.; Du, J.; Bai, L.; Sun, L. Highly Efficient Photoelectrochemical Water Splitting with an Immobilized Molecular Co4O4 Cubane Catalyst. *Angew. Chem. Int. Ed.* **2017**, *56*, 6911–6915. [CrossRef] [PubMed]
108. Zhang, Y.; Li, J.; Ma, L.; Cai, W.; Cheng, H. Recent Developments on Alternative Proton Exchange Membranes: Strategies for Systematic Performance Improvement. *Energy Technol.* **2015**, *3*, 675–691. [CrossRef]
109. Liu, Y.-L.; Su, Y.-H.; Chang, C.-M.; Suryani; Wang, D.-M.; Lai, J.-Y. Preparation and applications of Nafion-functionalized multiwalled carbon nanotubes for proton exchange membrane fuel cells. *J. Mater. Chem.* **2010**, *20*, 4409–4416. [CrossRef]
110. Murthy, A.P.; Theerthagiri, J.; Madhavan, J. Highly Water Dispersible Polymer Acid–Doped Polyanilines as Low-Cost, Nafion-Free Ionomers for Hydrogen Evolution Reaction. *ACS Appl. Energy Mater.* **2018**, *1*, 1512–1521. [CrossRef]
111. Johnson, B.A.; Bhunia, A.; Ott, S. Electrocatalytic water oxidation by a molecular catalyst incorporated into a metal-organic framework thin film. *Dalton Trans.* **2017**, *46*, 1382–1388. [CrossRef]
112. Buru, C.T.; Li, P.; Mehdi, B.L.; Dohnalkova, A.; Platero-Prats, A.E.; Browning, N.D.; Chapman, K.W.; Hupp, J.T.; Farha, O.K. Adsorption of a Catalytically Accessible Polyoxometalate in a Mesoporous Channel-type Metal-Organic Framework. *Chem. Mater.* **2017**, *29*, 5174–5181. [CrossRef]
113. Yamada, Y.; Oyama, K.; Gates, R.; Fukuzumi, S. High Catalytic Activity of Heteropolynuclear Cyanide Complexes Containing Cobalt and Platinum Ions: Visible-Light Driven Water Oxidation. *Angew. Chem. Int. Ed.* **2015**, *54*, 5613–5617. [CrossRef]
114. Yaghi, O.M.; O'Keeffe, M.; Ockwig, N.W.; Chae, H.K.; Eddaoudi, M.; Kim, J. Reticular synthesis and the design of new materials. *Nature* **2003**, *423*, 705–714. [CrossRef] [PubMed]
115. Lee, J.; Farha, O.K.; Roberts, J.; Scheidt, K.A.; Nguyen, S.T.; Hupp, J.T. Metal-organic framework materials as catalysts. *Chem. Soc. Rev.* **2009**, *38*, 1450–1459. [CrossRef] [PubMed]
116. Ashford, D.L.; Lapides, A.M.; Vannucci, A.K.; Hanson, K.; Torelli, D.; Harrison, D.; Templeton, J.L.; Meyer, T.J. Water Oxidation by an Electropolymerized Catalyst on Derivatized Mesoporous Metal Oxide Electrodes. *J. Am. Chem. Soc.* **2014**, *136*, 6578–6581. [CrossRef] [PubMed]
117. Hou, Y.; Cheng, Y.; Hobson, T.; Liu, J. Design and Synthesis of Hierarchical MnO2 Nanospheres/Carbon Nanotubes/Conducting Polymer Ternary Composite for High Performance Electrochemical Electrodes. *Nano Lett.* **2010**, *10*, 2727–2733. [CrossRef] [PubMed]
118. deKrafft, K.E.; Wang, C.; Xie, Z.; Su, X.; Hinds, B.J.; Lin, W. Electrochemical Water Oxidation with Carbon-Grafted Iridium Complexes. *ACS Appl. Mater. Interfaces* **2012**, *4*, 608–613. [CrossRef] [PubMed]
119. Lapides, A.M.; Sherman, B.D.; Brennaman, M.K.; Dares, C.J.; Skinner, K.R.; Templeton, J.L.; Meyer, T.J. Synthesis, characterization, and water oxidation by a molecular chromophore-catalyst assembly prepared by atomic layer deposition. The "mummy" strategy. *Chem. Sci.* **2015**, *6*, 6398–6406. [CrossRef]
120. Kirkland, J.J. Porous Thin-Layer Modified Glass Bead Supports for Gas Liquid Chromatography. *Anal. Chem.* **1965**, *37*, 1458–1461. [CrossRef]
121. Richardson, J.J.; Björnmalm, M.; Caruso, F. Technology-driven layer-by-ayer assembly of nanofilms. *Science* **2015**, *348*, aaa2491. [CrossRef]
122. Richardson, J.J.; Cui, J.; Björnmalm, M.; Braunger, J.A.; Ejima, H.; Caruso, F. Innovation in Layer-by-Layer Assembly. *Chem. Rev.* **2016**, *116*, 14828–14867. [CrossRef]
123. Borges, J.; Mano, J.F. Molecular Interactions Driving the Layer-by-Layer Assembly of Multilayers. *Chem. Rev.* **2014**, *114*, 8883–8942. [CrossRef]
124. Choi, Y.; Jeon, D.; Choi, Y.; Kim, D.; Kim, N.; Gu, M.; Bae, S.; Lee, T.; Lee, H.-W.; Kim, B.-S.; et al. Interface Engineering of Hematite with Nacre-like Catalytic Multilayers for Solar Water Oxidation. *ACS Nano* **2019**, *13*, 467–475. [CrossRef] [PubMed]
125. Decher, G. Fuzzy Nanoassemblies: Toward Layered Polymeric Multicomposites. *Science* **1997**, *277*, 1232–1237. [CrossRef]
126. Li, J.; Triana, C.A.; Wan, W.; Saseendran, D.P.A.; Zhao, Y.; Balaghi, S.E.; Heidari, S.; Patzke, G.R. Molecular and heterogeneous water oxidation catalysts: Recent progress and joint perspectives. *Chem. Soc. Rev.* **2021**, *50*, 2444–2485. [CrossRef] [PubMed]

127. Kunz, V.; Schmidt, D.; Röhr, M.I.S.; Mitrić, R.; Würthner, F. Supramolecular Approaches to Improve the Performance of Ruthenium–Based Water Oxidation Catalysts. *Adv. Energy Mater.* **2017**, *7*, 1602939. [CrossRef]
128. Li, W.; Sheehan, S.W.; He, D.; He, Y.; Yao, X.; Grimm, R.L.; Brudvig, G.W.; Wang, D. Hematite-Based Solar Water Splitting in Acidic Solutions: Functionalization by Mono-and Multilayers of Iridium Oxygen-Evolution Catalysts. *Angew. Chem. Int. Ed.* **2015**, *54*, 11428–11432. [CrossRef] [PubMed]
129. Sheehan, S.W.; Thomsen, J.M.; Hintermair, U.; Crabtree, R.H.; Brudvig, G.W.; Schmuttenmaer, C.A. A molecular catalyst for water oxidation that binds to metal oxide surfaces. *Nat. Commun.* **2015**, *6*, 6469. [CrossRef] [PubMed]
130. Liu, B.; Li, J.; Wu, H.-L.; Liu, W.-Q.; Jiang, X.; Li, Z.-J.; Chen, B.; Tung, C.-H.; Wu, L.-Z. Improved Photoelectrocatalytic Performance for Water Oxidation by Earth-Abundant Cobalt Molecular Porphyrin Complex-Integrated $BiVO_4$ Photoanode. *ACS Appl. Mater. Interfaces* **2016**, *8*, 18577–18583. [CrossRef]
131. Daniel, Q.; Duan, L.; Timmer, B.; Chen, H.; Luo, X.; Ambre, R.; Wang, Y.; Zhang, B.; Zhang, P.; Wang, L.; et al. Water Oxidation Initiated by In Situ Dimerization of the Molecular Ru(pdc) Catalyst. *ACS Catal.* **2018**, *8*, 4375–4382. [CrossRef]
132. Duan, L.; Fischer, A.; Xu, Y.; Sun, L. Isolated Seven-Coordinate Ru(IV) Dimer Complex with [HOHOH]-Bridging Ligand as an Intermediate for Catalytic Water Oxidation. *J. Am. Chem. Soc.* **2009**, *131*, 10397–10399. [CrossRef]
133. Sherman, B.D.; Xie, Y.; Sheridan, M.V.; Wang, D.; Shaffer, D.W.; Meyer, T.J.; Concepcion, J.J. Light-Driven Water Splitting by a Covalently Linked Ruthenium-Based Chromophore-Catalyst Assembly. *ACS Energy Lett.* **2017**, *2*, 124–128. [CrossRef]
134. Sato, S.; Iida, J.; Suzuki, K.; Kawano, M.; Ozeki, T.; Fujita, M. Fluorous Nanodroplets Structurally Confined in an Organopalladium Sphere. *Science* **2006**, *313*, 1273–1276. [CrossRef] [PubMed]
135. Tong, L.; Duan, L.; Xu, Y.; Privalov, T.; Sun , L. Structural Modifications of Mononuclear Ruthenium Complexes: A Combined Experimental and Theoretical Study on the Kinetics of Ruthenium-Catalyzed Water Oxidation. *Angew. Chem. Int. Ed.* **2011**, *50*, 445–449. [CrossRef] [PubMed]
136. Habisreutinger, S.N.; Leijtens, T.; Eperon, G.E.; Stranks, S.D.; Nicholas, R.J.; Snaith, H.J. Carbon Nanotube/Polymer Composites as a Highly Stable Hole Collection Layer in Perovskite Solar Cells. *Nano Lett.* **2014**, *14*, 5561–5568. [CrossRef]
137. Wee, K.-R.; Brennaman, M.K.; Alibabaei, L.; Farnum, B.H.; Sherman, B.; Lapides, A.M.; Meyer, T.J. Stabilization of Ruthenium(II) Polypyridyl Chromophores on Nanoparticle Metal-Oxide Electrodes in Water by Hydrophobic PMMA Overlayers. *J. Am. Chem. Soc.* **2014**, *136*, 13514–13517. [CrossRef] [PubMed]
138. Ding, X.; Gao, Y.; Ye, L.; Zhang, L.; Sun, L. Assembling Supramolecular Dye-Sensitized Photoelectrochemical Cells for Water Splitting. *ChemSusChem* **2015**, *8*, 3992–3995. [CrossRef]
139. Wang, D.; Wang, L.; Brady, M.D.; Dares, C.J.; Meyer, G.J.; Meyer, T.J.; Concepcion, J.J. Self-Assembled Chromophore-Catalyst Bilayer for Water Oxidation in a Dye-Sensitized Photoelectrosynthesis Cell. *J. Phys. Chem. C* **2019**, *123*, 30039–30045. [CrossRef]
140. Sévery, L.; Szczerbiński, J.; Taskin, M.; Tuncay, I.; Nunes, F.B.; Cignarella, C.; Tocci, G.; Blacque, O.; Osterwalder, J.; Zenobi, R.; et al. Immobilization of molecular catalysts on electrode surfaces using host-guest interactions. *Nat. Chem.* **2021**, *13*, 523–529. [CrossRef]
141. Cao, G.; Hong, H.G.; Mallouk, T.E. Layered metal phosphates and phosphonates: From crystals to monolayers. *Acc. Chem. Res.* **1992**, *25*, 420–427. [CrossRef]
142. Wang, D.; Xu, Z.; Sheridan, M.V.; Concepcion, J.J.; Li, F.; Lian, T.; Meyer, T.J. Photodriven water oxidation initiated by a surface bound chromophore-donor-catalyst assembly. *Chem. Sci.* **2021**, *12*, 14441–14450. [CrossRef]
143. Hoque, M.A.; Gil-Sepulcre, M.; de Aguirre, A.; Elemans, J.A.A.W.; Moonshiram, D.; Matheu, R.; Shi, Y.; Benet-Buchholz, J.; Sala, X.; Malfois, M.; et al. Water oxidation electrocatalysis using ruthenium coordination oligomers adsorbed on multiwalled carbon nanotubes. *Nat. Chem.* **2020**, *12*, 1060–1066. [CrossRef]
144. Garrido–Barros, P.; Gimbert–Suriñach, C.; Moonshiram, D.; Picón, A.; Monge, P.; Batista, V.S.; Llobet, A. Electronic π-Delocalization Boosts Catalytic Water Oxidation by Cu(II) Molecular Catalysts Heterogenized on Graphene Sheets. *J. Am. Chem. Soc.* **2017**, *139*, 12907–12910. [CrossRef] [PubMed]
145. Li, X.; Lei, H.; Liu, J.; Zhao, X.; Ding, S.; Zhang, Z.; Tao, X.; Zhang, W.; Wang, W.; Zheng, X.; et al. Carbon Nanotubes with Cobalt Corroles for Hydrogen and Oxygen Evolution in pH 0–14 Solutions. *Angew. Chem. Int. Ed. Engl.* **2018**, *57*, 15070–15075. [CrossRef] [PubMed]
146. Wang, C.; Xie, Z.; deKrafft, K.E.; Lin, W. Doping Metal-Organic Frameworks for Water Oxidation, Carbon Dioxide Reduction, and Organic Photocatalysis. *J. Am. Chem. Soc.* **2011**, *133*, 13445–13454. [CrossRef] [PubMed]
147. Lu, X.-F.; Liao, P.-Q.; Wang, J.-W.; Wu, J.-X.; Chen, X.-W.; He, C.-T.; Zhang, J.-P.; Li, G.-R.; Chen, X.-M. An Alkaline-Stable, Metal Hydroxide Mimicking Metal-Organic Framework for Efficient Electrocatalytic Oxygen Evolution. *J. Am. Chem. Soc.* **2016**, *138*, 8336–8339. [CrossRef] [PubMed]
148. Manna, P.; Debgupta, J.; Bose, S.; Das, S.K. A Mononuclear CoII Coordination Complex Locked in a Confined Space and Acting as an Electrochemical Water-Oxidation Catalyst: A "Ship-in-a-Bottle" Approach. *Angew. Chem. Int. Ed.* **2016**, *55*, 2425–2430. [CrossRef]
149. Wang, S.; Hou, Y.; Lin, S.; Wang, X. Water oxidation electrocatalysis by a zeolitic imidazolate framework. *Nanoscale* **2014**, *6*, 9930–9934. [CrossRef]
150. Wurster, B.; Grumelli, D.; Hötger, D.; Gutzler, R.; Kern, K. Driving the Oxygen Evolution Reaction by Nonlinear Cooperativity in Bimetallic Coordination Catalysts. *J. Am. Chem. Soc.* **2016**, *138*, 3623–3626. [CrossRef]

151. Dogutan, D.K.; McGuire, R.; Nocera, D.G. Electocatalytic Water Oxidation by Cobalt(III) Hangman β-Octafluoro Corroles. *J. Am. Chem. Soc.* **2011**, *133*, 9178–9180. [CrossRef]
152. Moss, J.A.; Yang, J.C.; Stipkala, J.M.; Wen, X.; Bignozzi, C.A.; Meyer, G.J.; Meyer, T.J. Sensitization and Stabilization of TiO_2 Photoanodes with Electropolymerized Overlayer Films of Ruthenium and Zinc Polypyridyl Complexes: A Stable Aqueous Photoelectrochemical Cell. *Inorg. Chem.* **2004**, *43*, 1784–1792. [CrossRef]
153. Lapides, A.M.; Ashford, D.L.; Hanson, K.; Torelli, D.A.; Templeton, J.L.; Meyer, T.J. Stabilization of a Ruthenium(II) Polypyridyl Dye on Nanocrystalline TiO2 by an Electropolymerized Overlayer. *J. Am. Chem. Soc.* **2013**, *135*, 15450–15458. [CrossRef]
154. Ashford, D.L.; Sherman, B.D.; Binstead, R.A.; Templeton, J.L.; Meyer, T.J. Electro-assembly of a Chromophore-Catalyst Bilayer for Water Oxidation and Photocatalytic Water Splitting. *Angew. Chem. Int. Ed.* **2015**, *54*, 4778–4781. [CrossRef] [PubMed]
155. Leem, G.; Sherman, B.D.; Burnett, A.J.; Morseth, Z.A.; Wee, K.-R.; Papanikolas, J.M.; Meyer, T.J.; Schanze, K.S. Light-Driven Water Oxidation Using Polyelectrolyte Layer-by-Layer Chromophore-Catalyst Assemblies. *ACS Energy Lett.* **2016**, *1*, 339–343. [CrossRef]